The Abdus Salam
International Centre for Theoretical Physics

United Nations
Educational, Scientific
and Cultural Organization

International Atomic
Energy Agency

SMR: 1643/11

WINTER COLLEGE ON OPTICS ON OPTICS AND PHOTONICS IN NANOSCIENCE AND NANOTECHNOLOGY

(7 - 18 February 2005)

"Surface-Enhanced Raman Scattering"

presented by:

Martin Moskovits
University of California,
Santa Barbara, U.S.A.

These are preliminary lecture notes, intended only for distribution to participants.

Lecture 1: Rough Silver

Peter McBreen, Professor of Chemistry Laval U

Jung Sang Suh, Professor of Chemistry Seoul NU

Ding Ping Tsai, Professor of Physics, Taiwan NU

Vladimir Shalaev, Professor of EE, Purdue

Bob Wolkow, Professor of Physics, U of Alberta

Constantine Douketis, Business tycoon

LinLin Tay, National Research Council of Canada

DaeHong Jeong, Professor of Chemistry Education, Seoul NU

Dr. Ioana Pavel

Collaborators: Prof. Blanka Vlckova, Charles University, Prague, Prof. Kevin Plaxco

ICTP Winter College in Optics and Photonics in Nano S&T

Some background

1976 -- Fleischman and coworkers (Southampton) observe unusually intense Raman scattering from pyridine adsorbed on electrochemically roughened silver. They ascribe the intensity to the increased surface area.

1977 -- Rick Van Duyne (Northwestern) and Alan Creighton (Kent) repeat these measurements and conclude that the enhancement is ~10^5 - 10^6 -- much too large to account for, by the increased surface area alone.

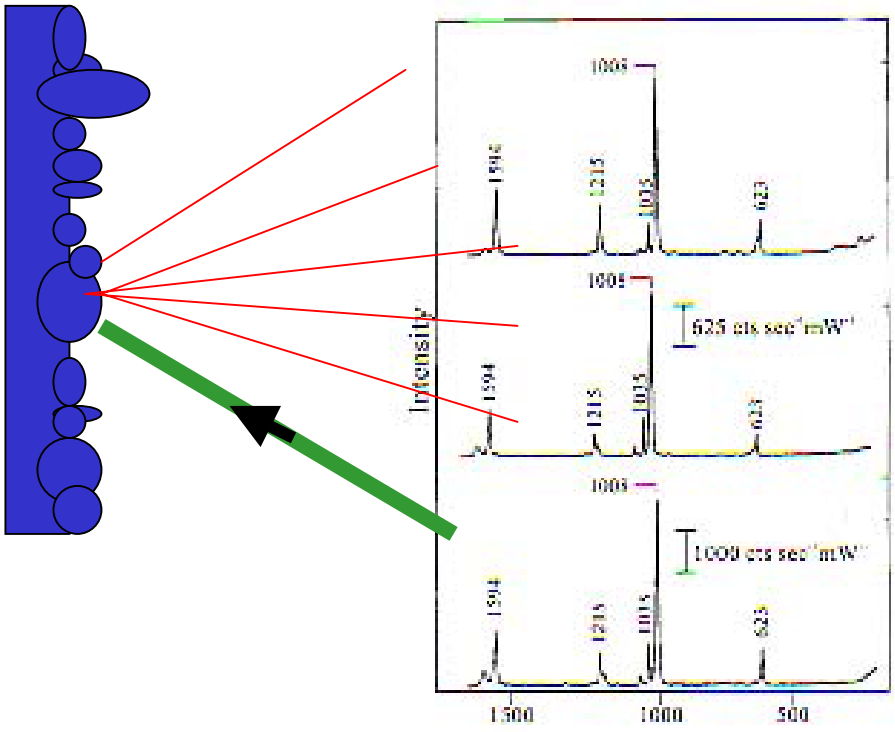

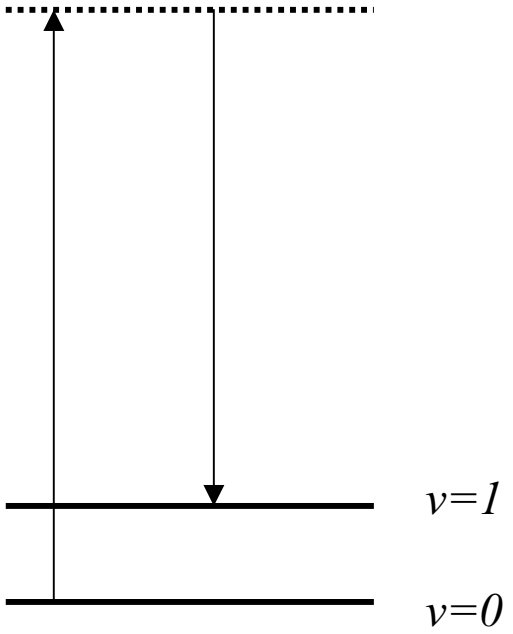

SERS seemed to have several common characteristics

- It required nanostructured metal
- Only a few metals seemed to produce very strong enhancements (Ag, Au, alkalis, less so with Pt, Al, In)
- It was a resonant process (some wavelengths worked well, others not)
- The molecule didn't have to be adsorbed on the metal, but there was extra enhancement when it was.

But multi-particle effects overwhelm single-particle signals. This is why single-particle excitation spectra have not been conclusively reported.

Most SERS-active systems are, in-fact, systems of interacting particles with enhancements significantly larger that that of single particles.

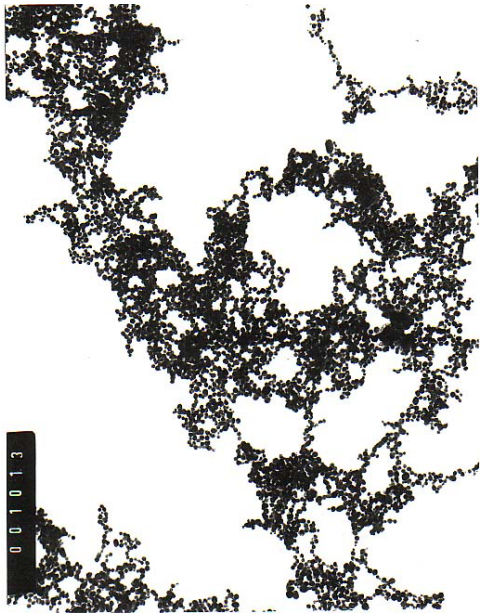

Colloid cluster

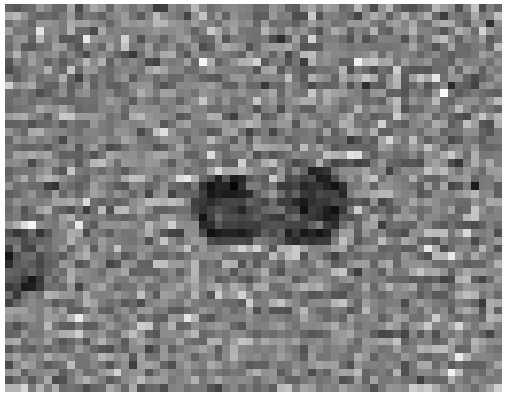

Dimers and other small clusters of nanoparticles

Rough surfaces possessing small, closely coupled features

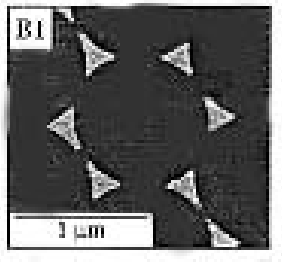

High-enhancement can also be achieved with particles if appropriate geometry. E.g. prolate ellipsoids or VanDuyne's triangular particles produced using nanosphere lithography.

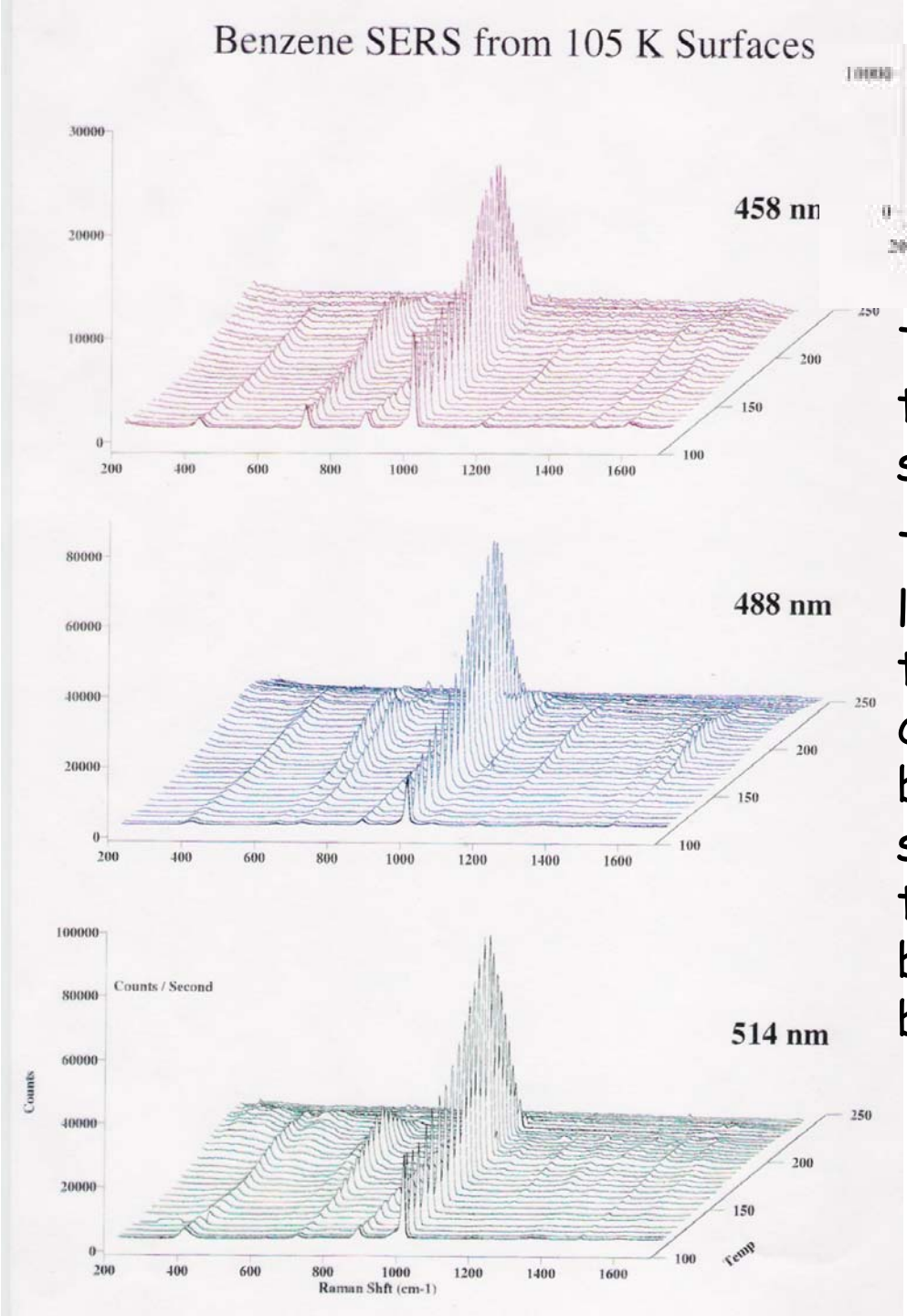

These two band, the second and third-most intense bands in the spectrum, are Raman forbidden.

This may be due to symmetry-lowering due to adsorption. But the small frequency shifts compared with solution-phase benzene makes it unlikely that such intense bands result from the small deformation of the benzene molecule due to its bonding to the Ag surface

The Raman selection rules are determined by the condition that the induced transition dipole between the initial and final states belong to the totally symmetrical representation. . Because the ground state if often totally symmetric, this means that the excited state vibration must span the same representation that also spans μ. And since the expression for μ, is normally truncated at , the Raman active modes are those that span the same irreducible representations as components of α. Now the polarizability is a second rank tensor that transforms as products of two translations, and because (classically) it arises from the summation of the distances of charges of the molecule, the magnitude of its components are of the order of $\sim a_M^2$, where a_M is ~ the molecular dimension.

In general, the expression for μ is an infinite series in which the third term is , in which *A* is a third rank tensor that transforms as the product of three translations. The dyadic of the field (in the far field), in rough terms can be written . Hence the ratio of the third term to that of the second term in the far field is $= \sim 2\pi a_M/\lambda$. Molecular sizes are ~1/500 of the size of wavelengths. Hence, in the far field one normally doesn't see modes enabled by the third term of the above equation.

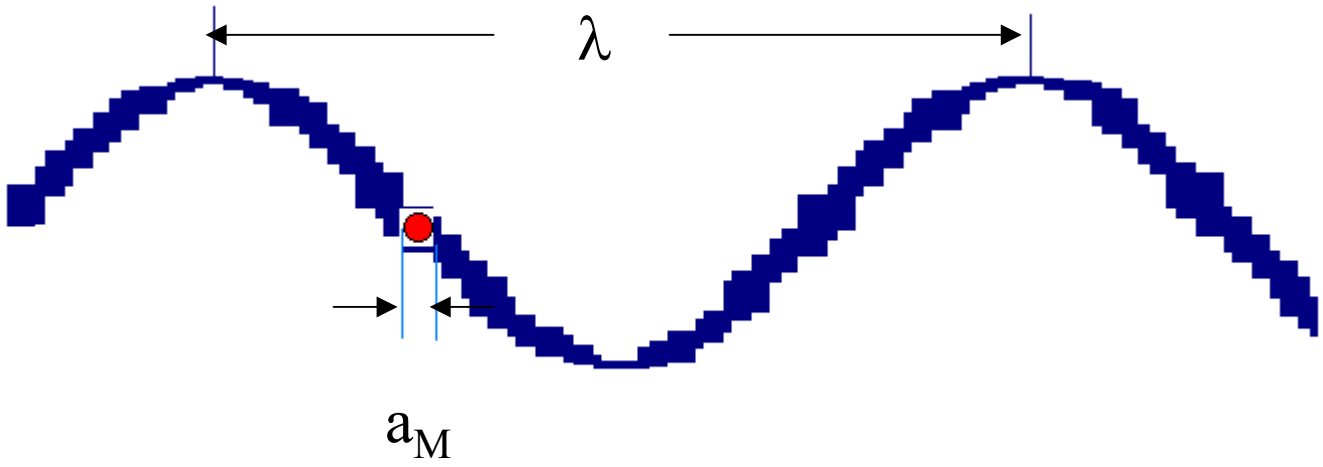

But near a metal surface all this is changed. The field inside the metal falls rapidly to zero hence the rate of change of field intensity near the metal is large and the ratio of the above terms becomes ~ a_M/a_S, where a_S is the distance over which the field drops by a unit measure near the surface. Hence vibrational modes that transform as the product of three translations become Raman active for molecules near metal surfaces.

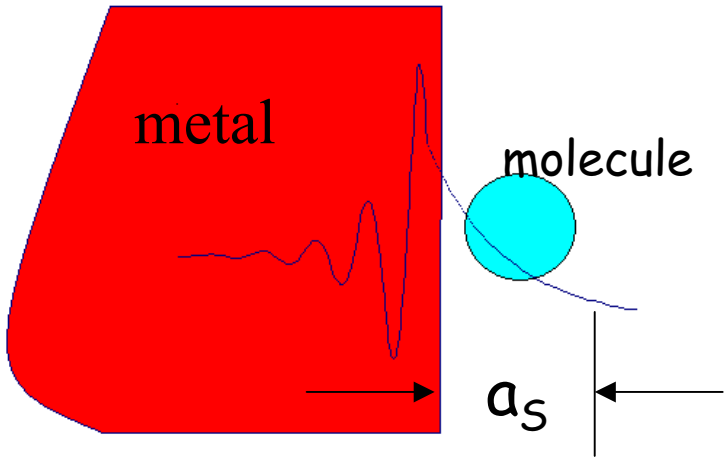

The properties of cold-quenched films

These show: (i) SERS (ii) enhanced photochemistry
(iii) enhanced non-linear effects (iv) etc.

conventional wisdom: if they are deposited at a low enough T they are randomly rough

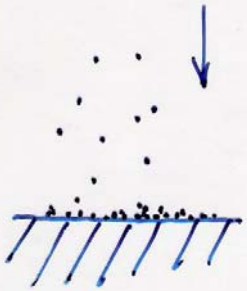

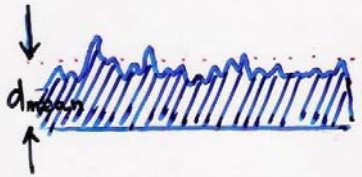

Random hill & void model

on illumination high field sites are at various locations

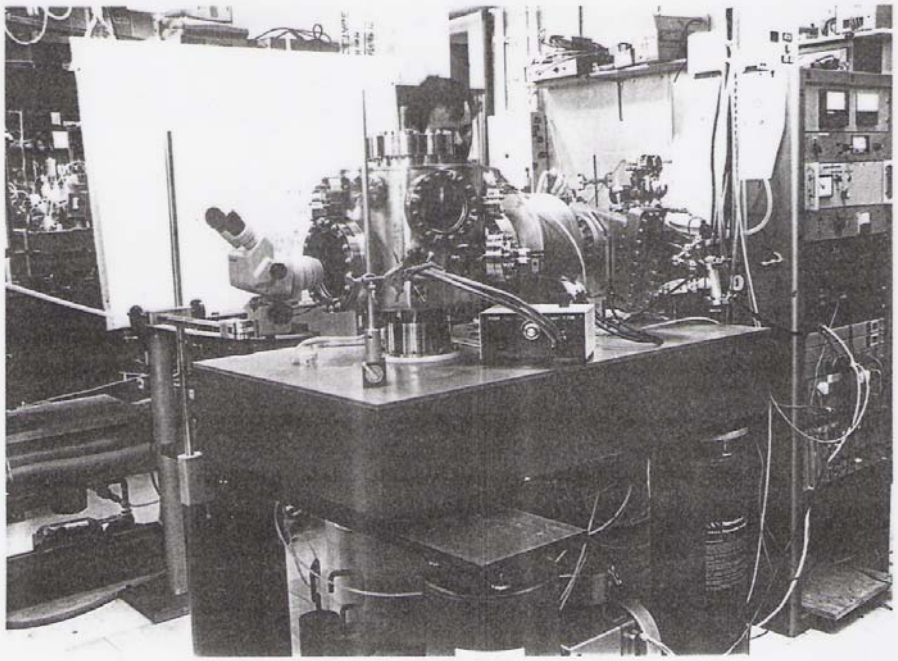

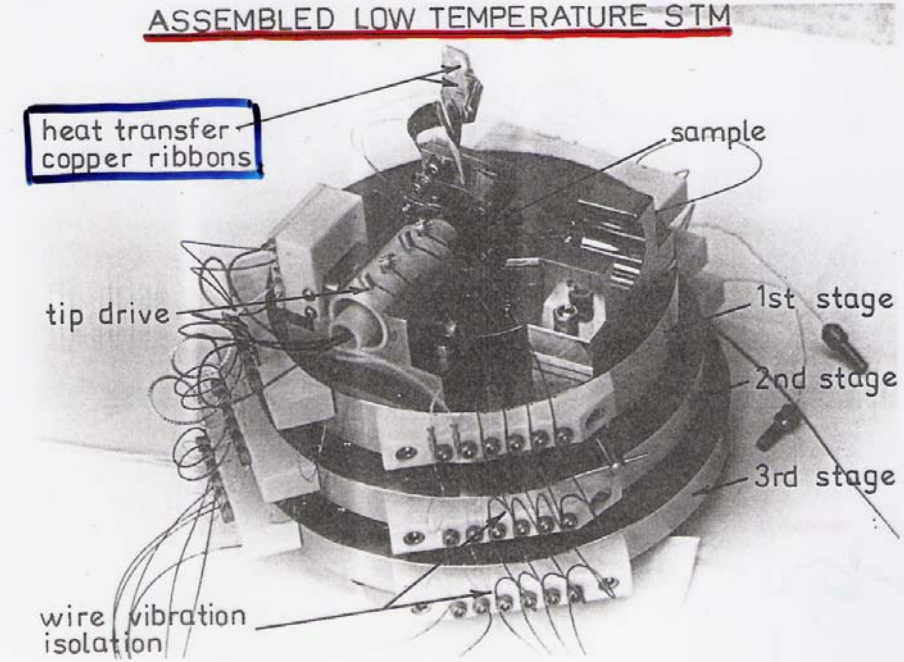
ASSEMBLED LOW TEMPERATURE STM
heat transfer copper ribbons
sample
tip drive
1st stage
2nd stage
3rd stage
wire vibration isolation

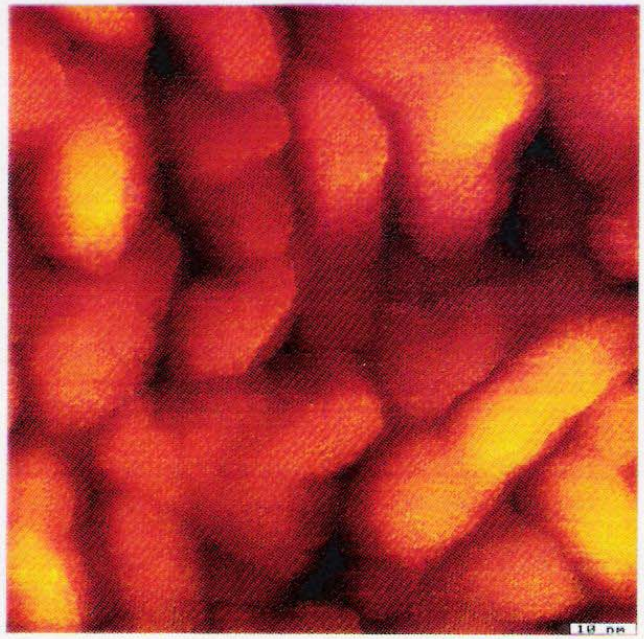

250 K

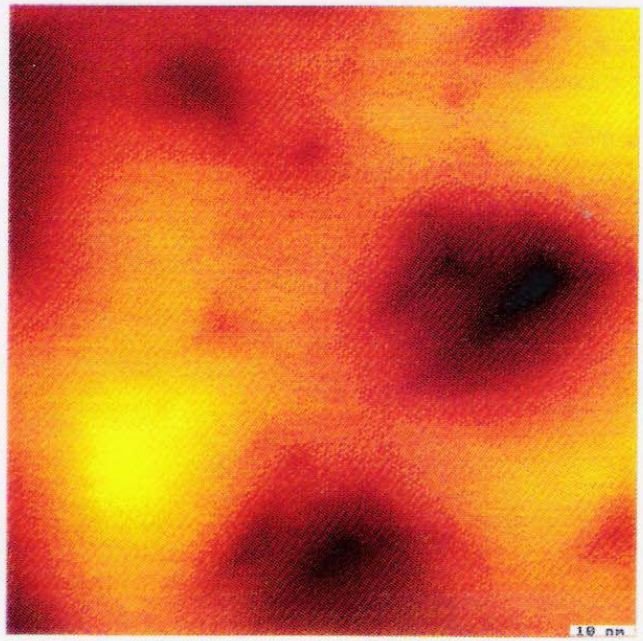

300 K

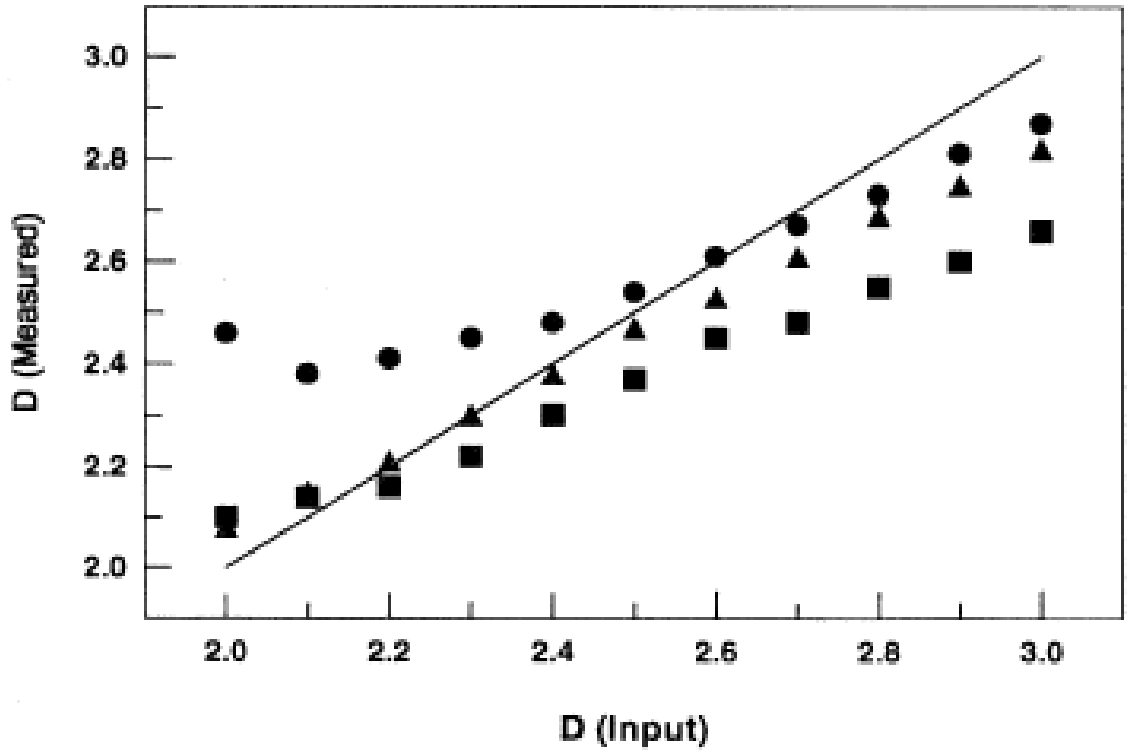

FIG. 7. Comparison of the local fractal dimension D(measured), calculated for numerically generated fractal surfaces as a function of D(input), the fractal dimension assumed in the simulation. Circles refer to the values of D calculated using power spectrum analysis, triangles to triangulation, and squares to cube counting.

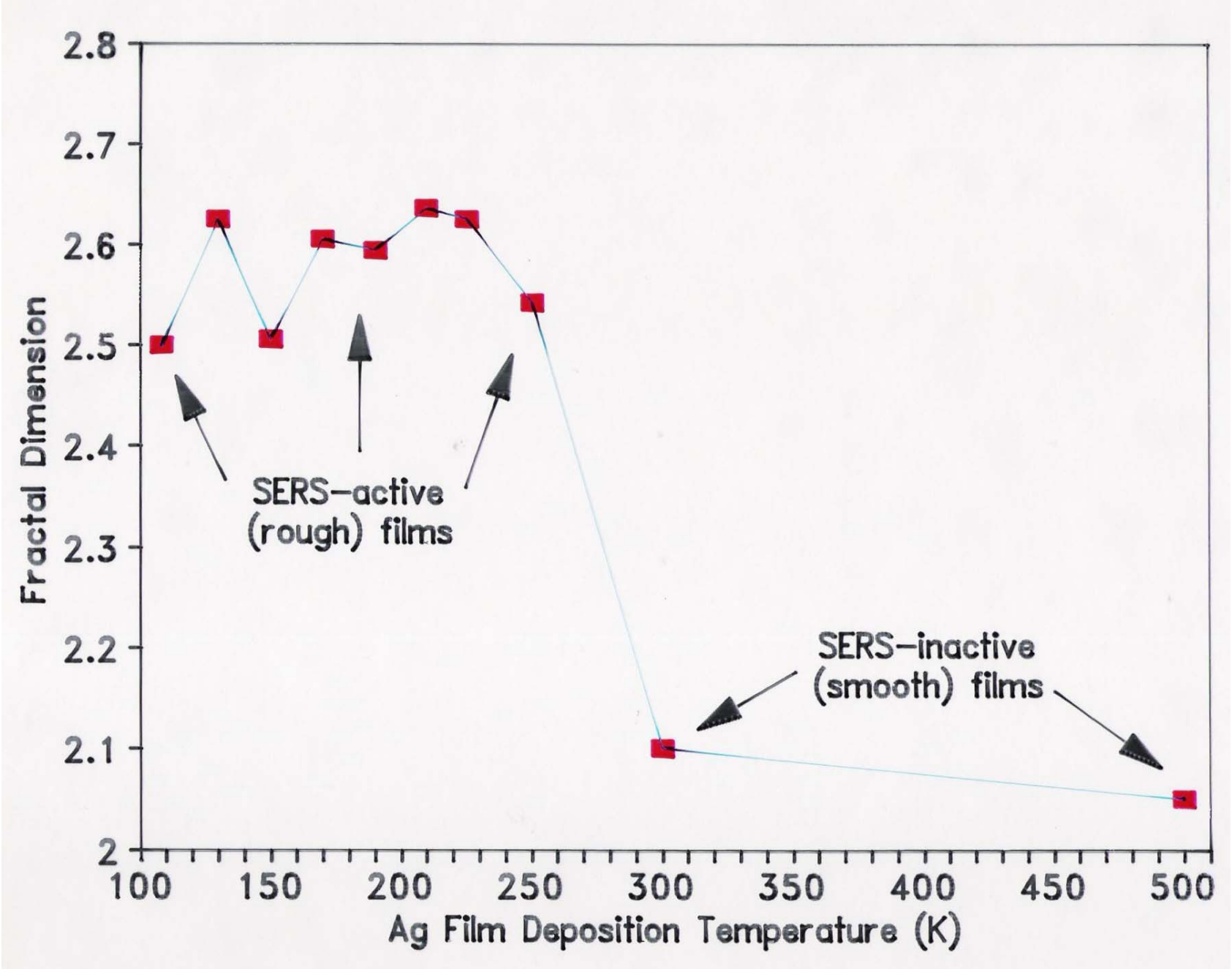
2.8
2.7
2.6
2.5
2.4
2.3
2.2
2.1
2
Fractal Dimension
SERS–active
(rough) films
SERS–inactive
(smooth) films
100
150
200
250
300
350
400
450
500
Ag Film Deposition Temperature (K)

Standard deviation of height $\xi(L) = \left[\langle H(\vec{r})^2 \rangle - \langle H(\vec{r}) \rangle^2 \right]^{1/2}$ "thickness of the surface"

is often found to follow a relationship:

$\xi(L,t) \sim t^{\beta}$ for $t/L^{\alpha/\beta} \ll 1$ (early times, large scale)

$\xi(L,t) \sim L^{\alpha}$ for $t/L^{\alpha/\beta} \gg 1$ (late times, small scale)

up to $L = L_c$ above which $\xi = \delta$

for continuous growth $t \propto \langle H \rangle$

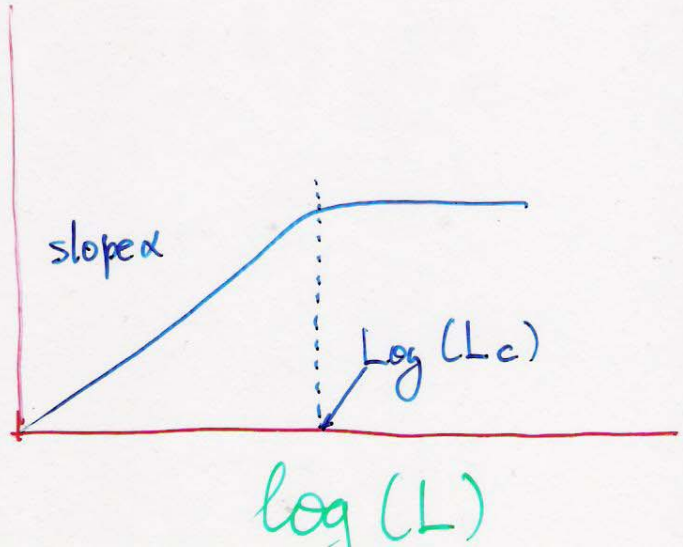

Simulations of growing self-affine surfaces

(1) Monte Carlo and MD calculations still limited by sample set accessible

(2) Empirical Continuum Equations

		α	β
(i)	stochastic growth: $\frac{\partial H}{\partial t} = \eta(\vec{r},t)$	0	1/2
(ii)	Kardar, Parisi, Zhang (KPZ) eq. $\frac{\partial H}{\partial t} = \nu \nabla^2 H + \frac{\lambda}{2}(\nabla H)^2 + \eta(\vec{r},t)$	~0.4	~0.25
(iii)	$\lambda = 0$	0	0
(iv)	Wolf, Villain eq. $\frac{\partial H}{\partial t} = -\omega \nabla^4 H + \eta(\vec{r},t)$	1	1/4
(v)	Additional non-linear term $\frac{\partial H}{\partial t} = -\omega \nabla^4 H + \rho \nabla^2 (\nabla H)^2 + \eta(\vec{r},t)$	2/3	1/5

$\nu \nabla^2 H$: hills erode, valleys fill in

$\frac{\lambda}{2}(\nabla H)^2$: non-linear term preserves rotational symmetry

$\Rightarrow$ self-similar

$-\omega \nabla^4 H$: approximates surface diffusion

$\rho \nabla^2 (\nabla H)^2$: approximates the action of steps as sources and sinks of atoms

α, β independent of T

None of these continuum equations can predict epitaxial layer by layer growth.

A value of $\alpha = 0.4$ is also what one normally calculates (and obtains experimentally) for metal on metal growth. The fractal dimension measured for our rough films (2.6) correspond to a value of $\alpha = 0.4$

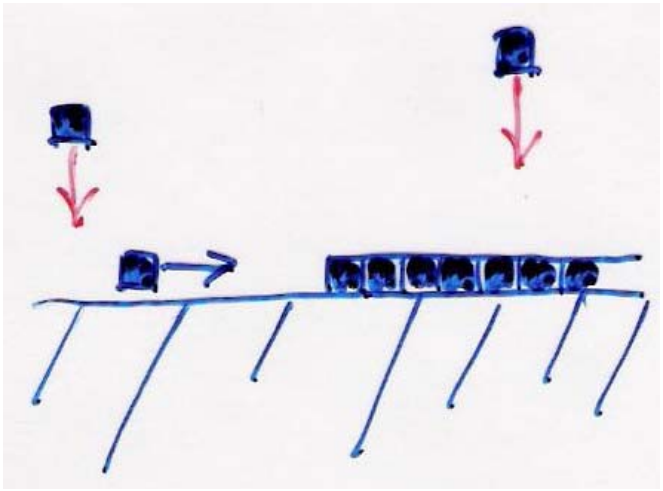

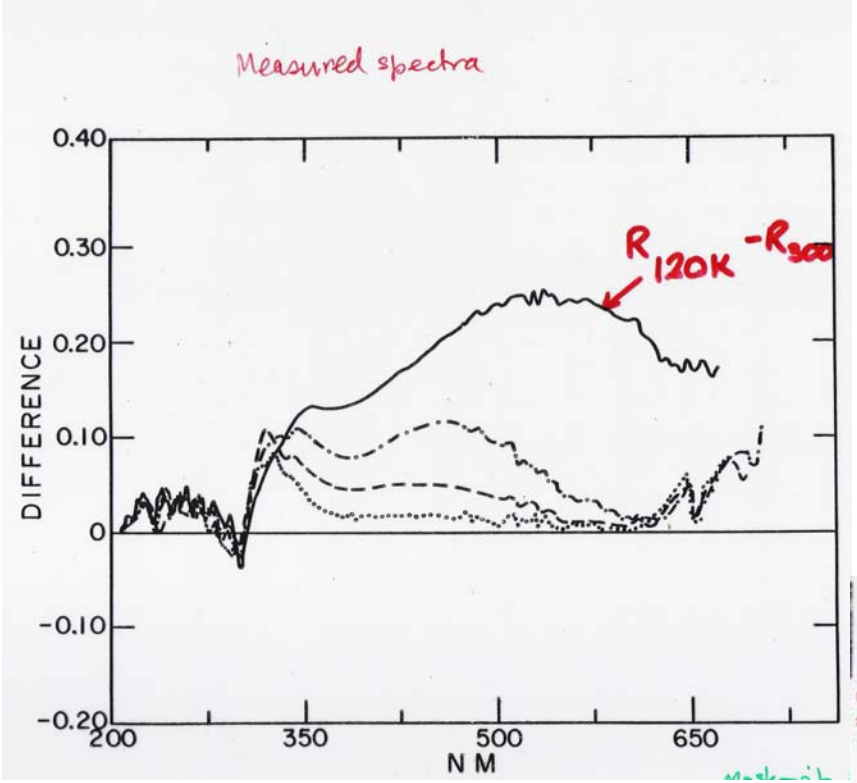

How is this structure related to Optics and photonics?

Ellipsometric spectroscopy of cold-deposited silver film,

McBreen et al J. Appl. Phys. 54 329 (1983)

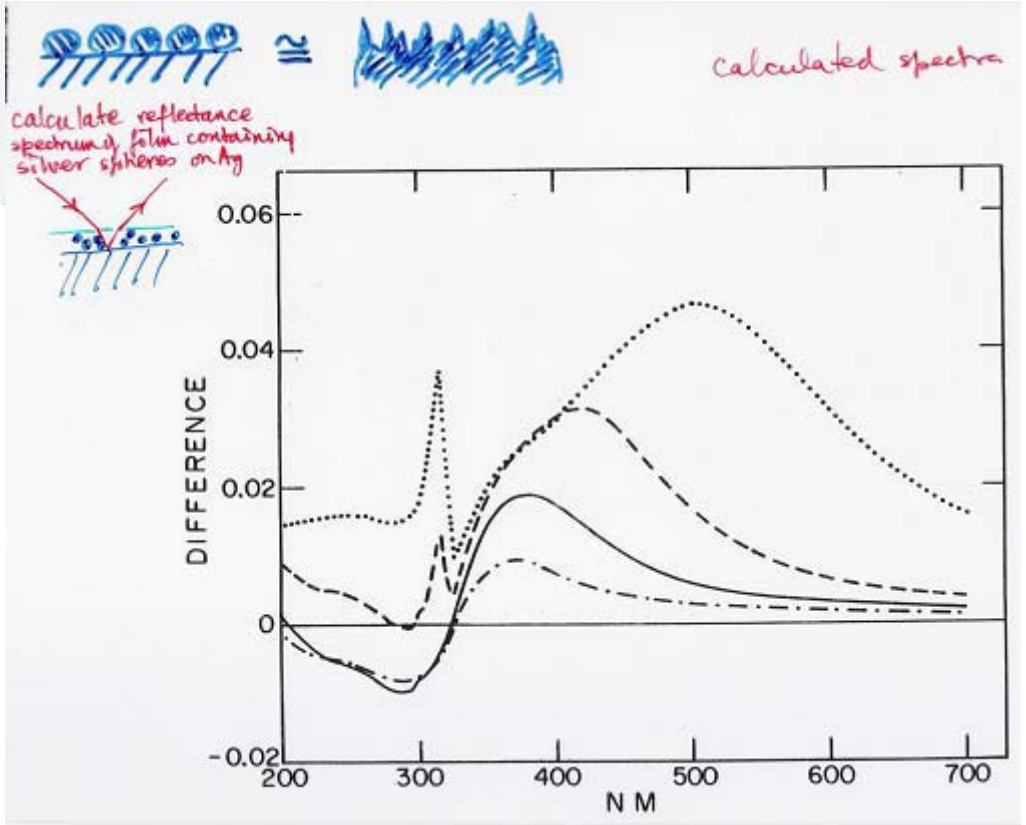

How well does a nano-rough silver surface approximate a layer of silver nanoparticles deposited on a smooth silver substrate, optically?

Two Experiments

1-photon

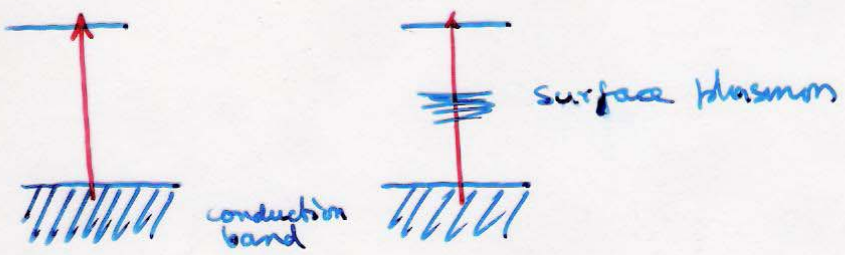

smooth rough

doubled excimer-pumped dye

2-photon

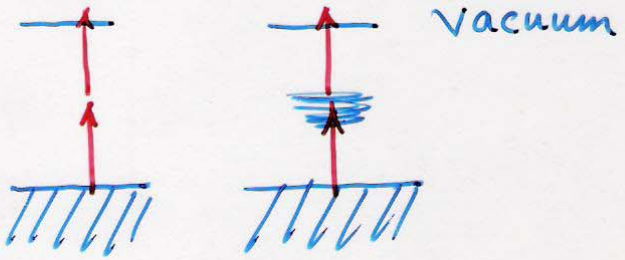

smooth rough

excimer-pumped dye

as a function of $\hbar\omega$ (or $2\hbar\omega$) near threshold.

Yield should depend on $\hbar\omega$ as:

$$Y_1 = A_1(\hbar\omega - \phi)^2 \quad \text{or} \quad Y_2 = A_2(2\hbar\omega - \phi)^2$$

(Fowler relation)

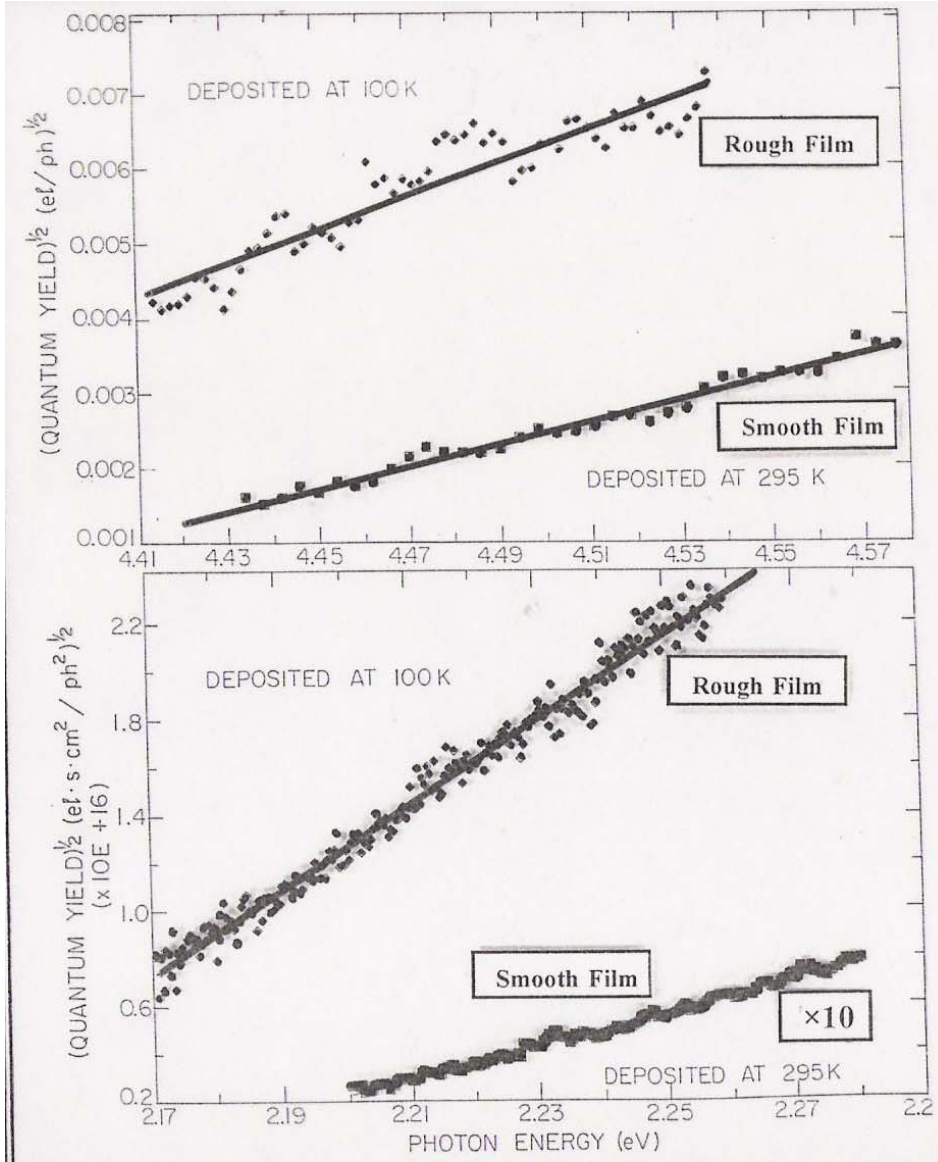

$$QY^{1P} = \frac{J\left(\frac{electrons}{cm^2\,s}\right)}{I\left(\frac{photons}{cm^2\,s}\right)} = A_1 \times (\hbar\omega' - \Phi)^2$$

$$A_1^{Rough} \sim A_1^{Smooth} \sim 10^{-4}\left(\frac{electrons}{photons\,eV^2}\right)$$

$$QY^{2P} = \frac{J\left(\frac{electrons}{cm^2\,s}\right)}{I^2\left(\frac{photons}{cm^2\,s}\right)^2} = A_2 \times (2\hbar\omega - \Phi)^2$$

$$A_2^{Smooth} \sim 10^{-33}\left(\frac{electron}{photon\,eV^2}\right)\left(\frac{cm^2\,s}{photon}\right)$$

$$A_2^{Rough} \sim 10^{-30}\left(\frac{electron}{photon\,eV^2}\right)\left(\frac{cm^2\,s}{photon}\right)$$

The 2-photon electron emission Quantum Yield from rough films is enhanced approximately 1000-fold compared to smooth films due to the involvement of Localized Surface Plasmons.

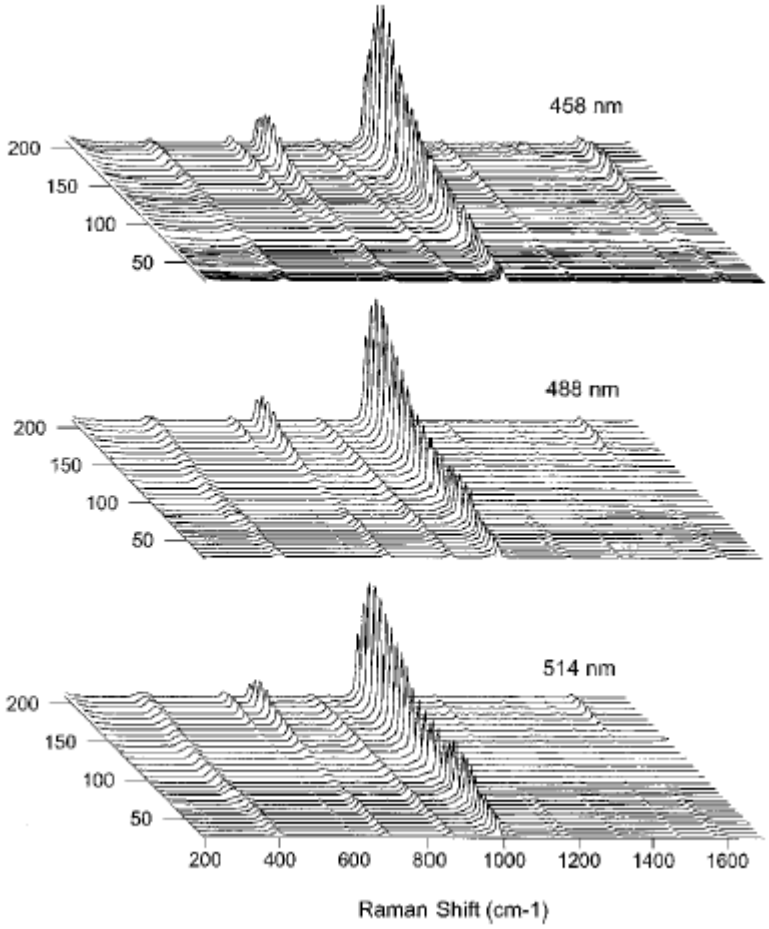

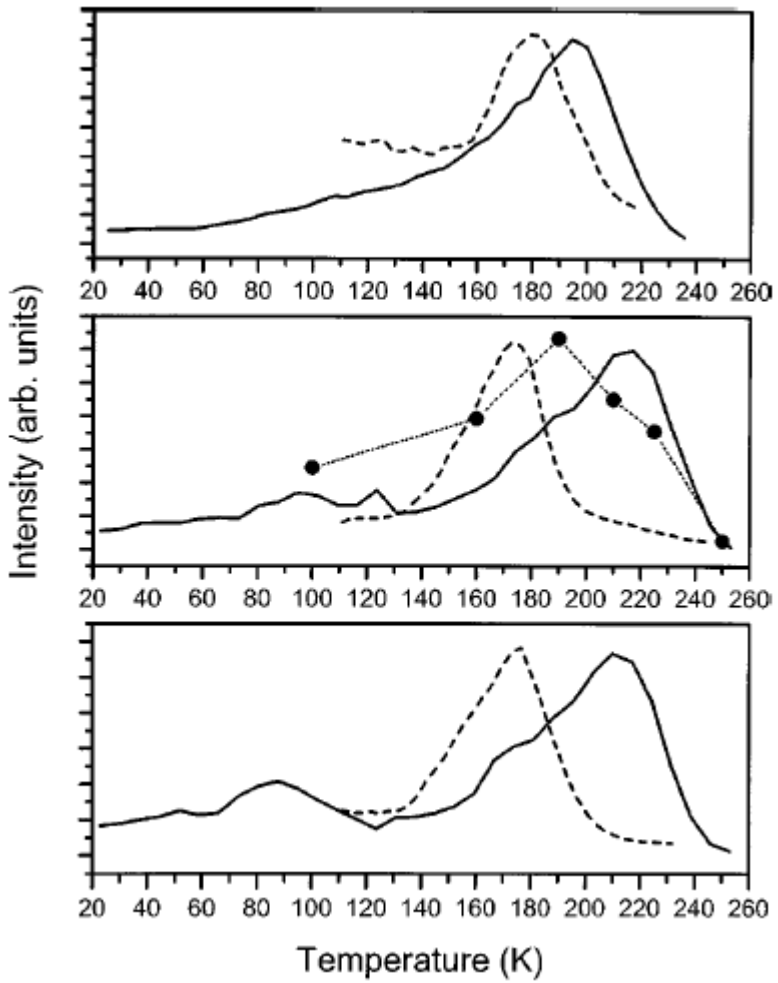

There are resonances involved,

Douketis et al J. Chem. Phys. 113, 11315 (2000)

$$\alpha = R^3 \frac{\varepsilon - 1}{\varepsilon + 2} \qquad \varepsilon = \varepsilon_b + 1 - \frac{\omega_p^2}{\omega^2 + i\omega\gamma}$$

$$\alpha = \frac{R^3(\varepsilon_b \omega^2 - \omega_p^2) + i\omega\gamma\varepsilon_b}{((\varepsilon_b + 3)\omega^2 - \omega_p^2) + i\omega\gamma(\varepsilon_b + 3)}$$

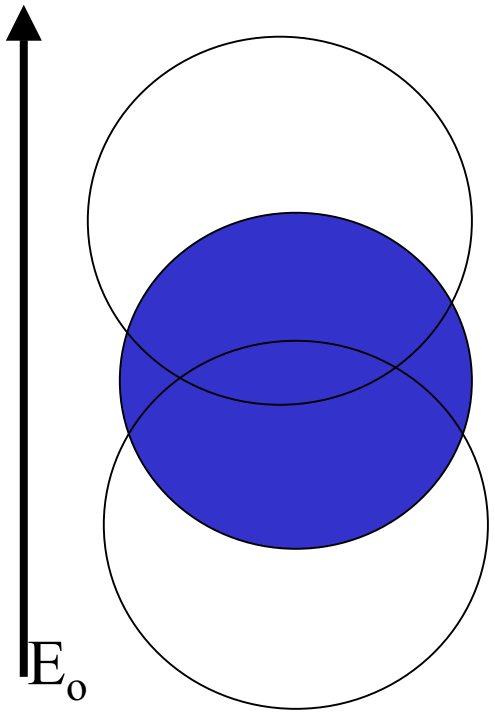

$$\omega_R = \frac{\omega_p}{\sqrt{\varepsilon_b + 3}}$$

For a small particle with radius much smaller than the wavelength, the oscillating incident field induces only a dipole whose magnitude is given by αE_o. The expression for the polarizability of the dielectric sphere has a pole at a frequency ω_R. The resonance can be very sharp when the sphere is very conductive and free from interband transitions.

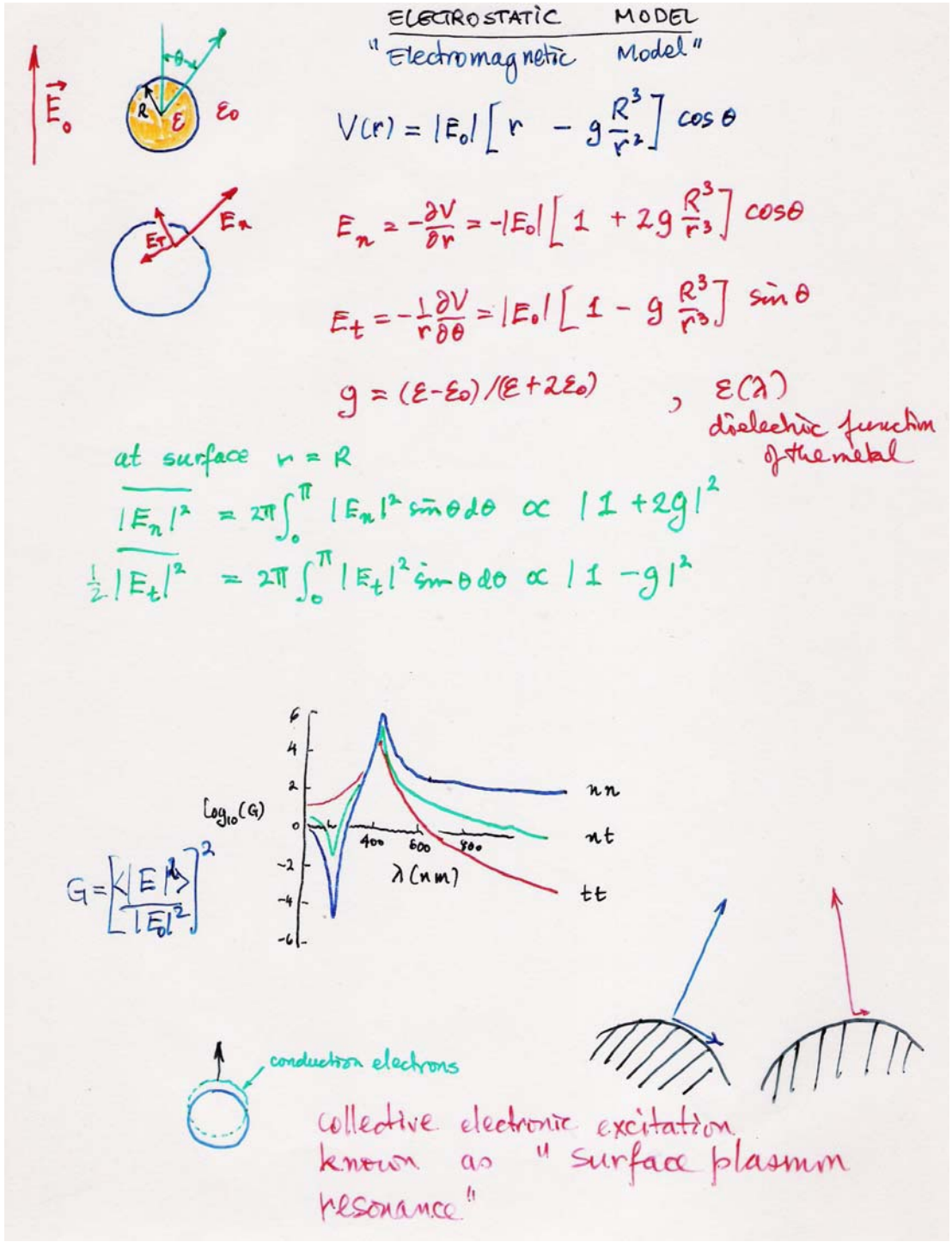

Molecular orientation determination: For a symmetric molecule that adsorbs on the surface in an oriented fashion so that one of its axes of symmetry corresponds to the surface normal (call it z), those modes that belong to the same irreducible representation as z^2 does will be preferentially enhanced as one proceeds towards the red.

Käll and Xu

Basic electromagnetic theory of SERS: the em field enhancement, β, enters as β^4 although the enhanced Raman intensity is proportional to E_o^2, that is, to the incident intensity. SERS is, therefore, a linear effect despite the β^4 dependence.

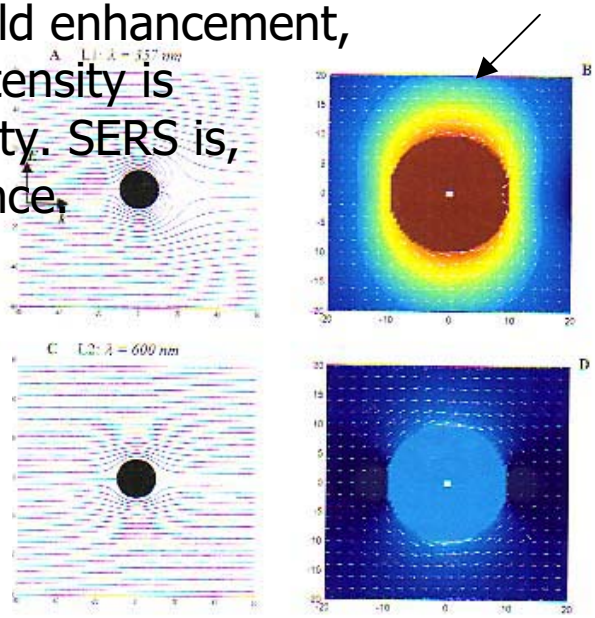

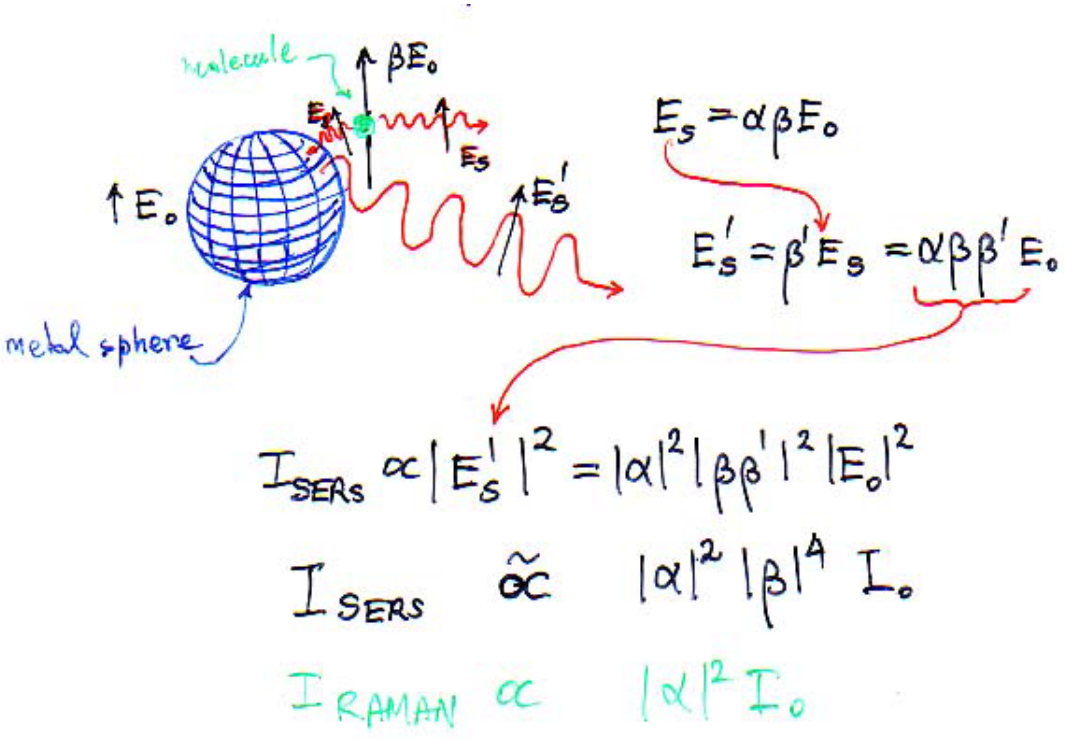

The enhancement both of the incident and Raman-scattered field comes out of the redistribution of the incident em energy surrounding the particle.

Enhancement, $G=I_{SERS}/I_{Raman} \sim \beta^4$ for small Stokes shift and $\sim \beta^{2\text{-}4}$ for very large Stokes shifts.

Nanostructural details of the optical response of a fractal silver cluster or a self-affine nano-rough silver film

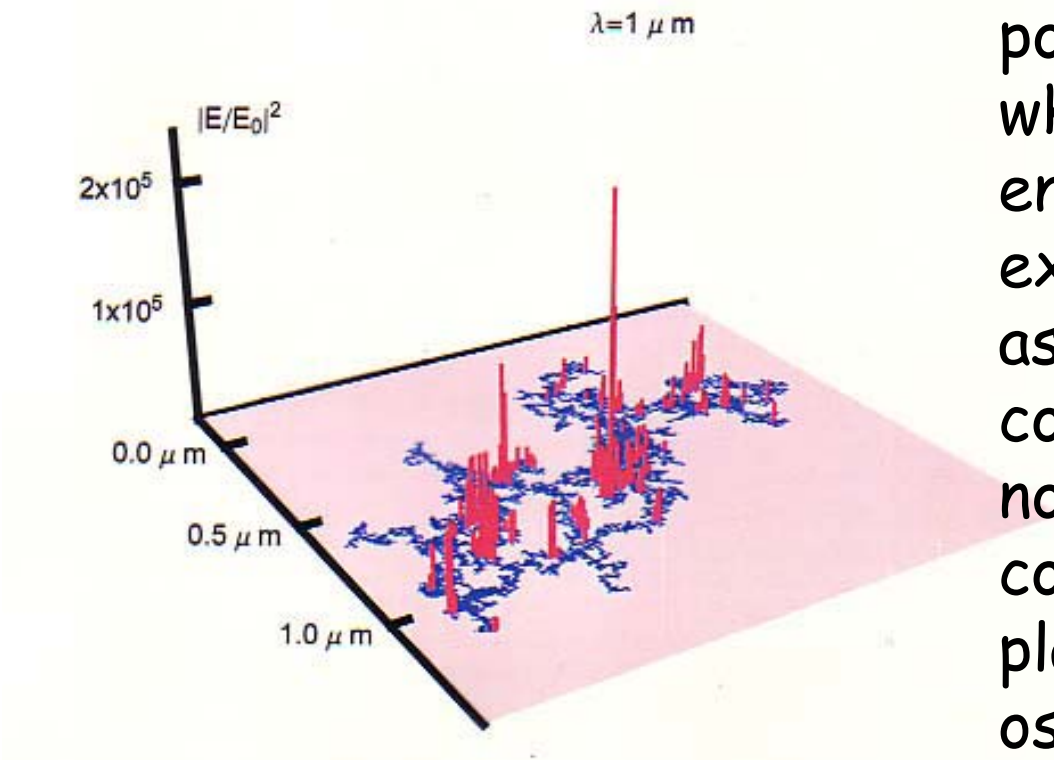

Stockman et al.

Shalaev et al.

Fractal clusters of nanoparticles excited in the surface plasmon region are predicted to possess "hot spots" where the SERS enhancement is expected to be as large as 10^{11}. These hot spots correspond to localized normal modes of coupled, dipolar surface plasmons, each oscillator resident on a nanoparticle.

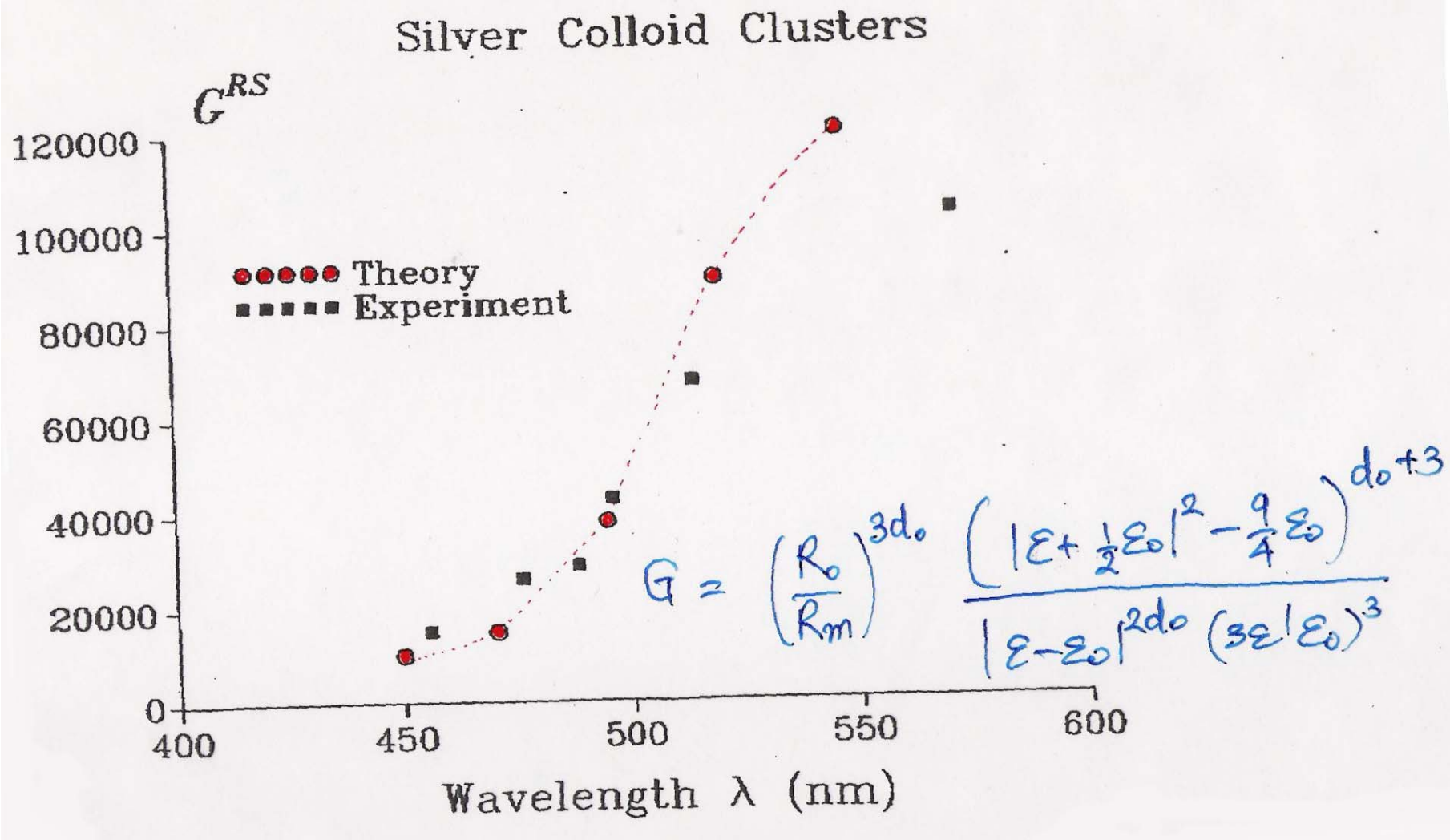

Stockman et al, PRB, 1992

Corroborative observations by near-field microscopy

TOPOGRAPHIC AND OPTICAL

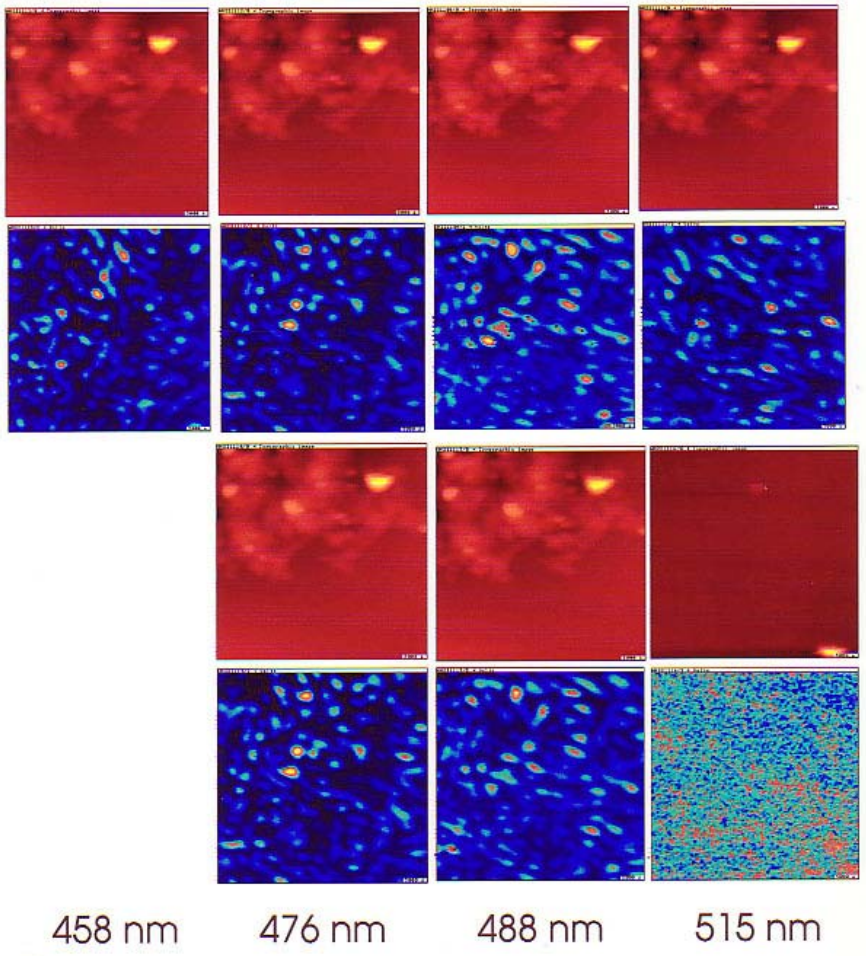

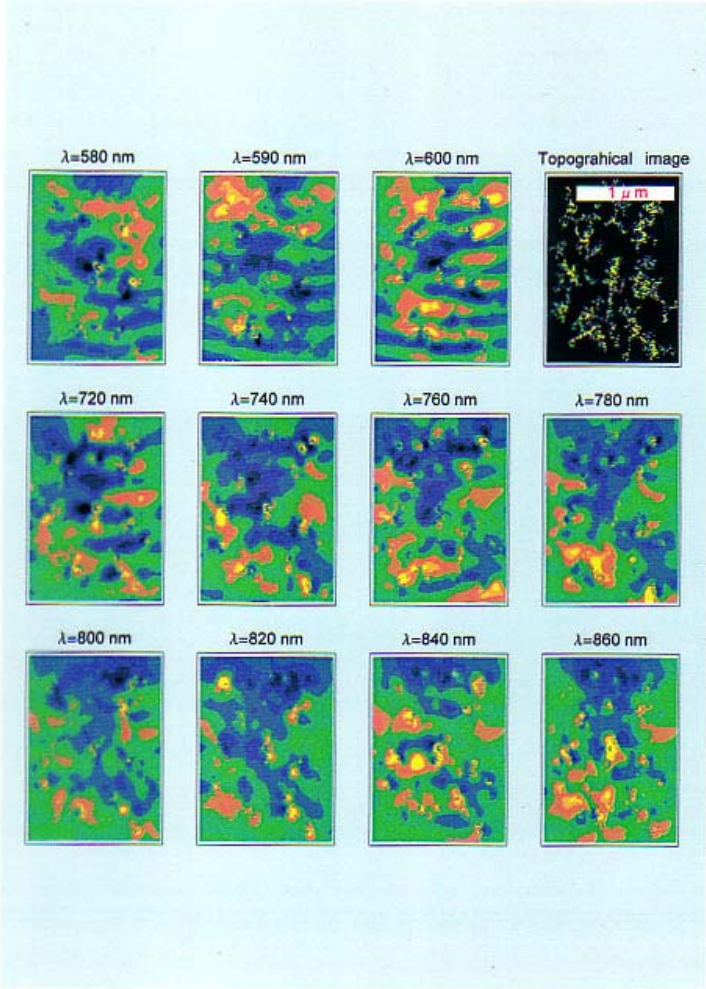

Hot spot activity observed in fractal aggregates of nanoparticles by near-field microscopy (Tay et al) is in close agreement with what is predicted using discrete dipole approximation (Shalaev, Markel).

Tay, Huynh and Zhang

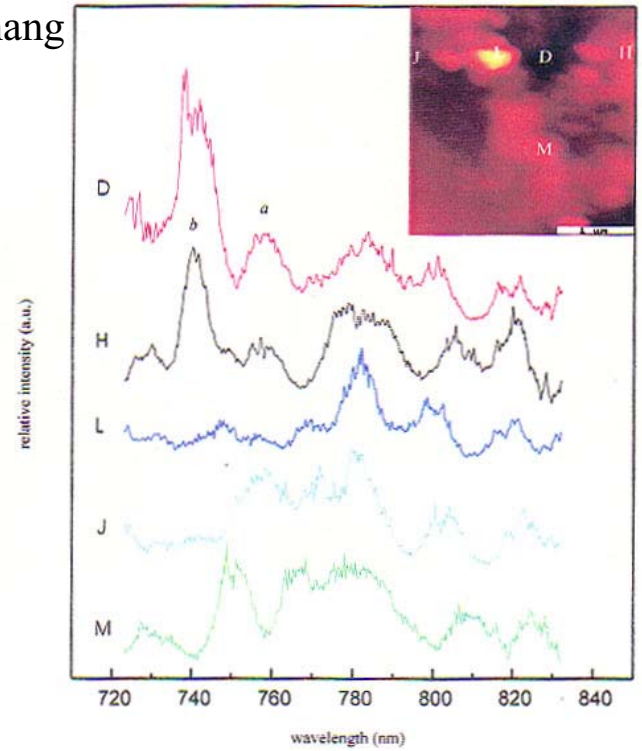

Observed

Calculated

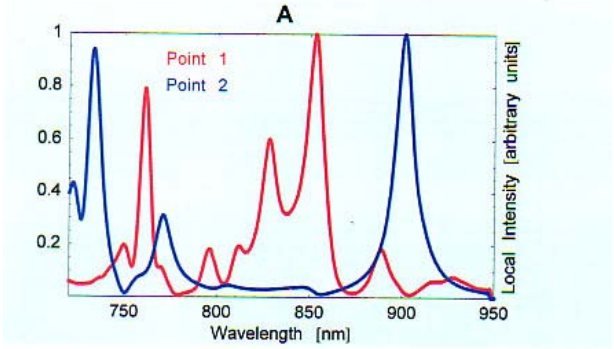

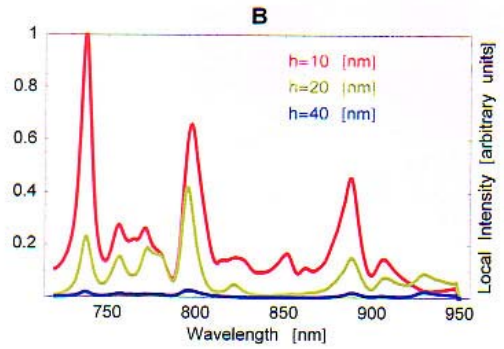

Shalaev and Markel

Near-field Rayleigh excitation spectra of fractal nanoparticle aggregate show strong evidence of individual plasmon normal modes. These are almost totally washed washed out in the far field.

Near-Field Raman Maps of Phthalazine on Ag Film

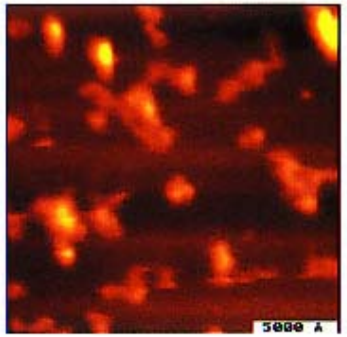

Shear force topography image

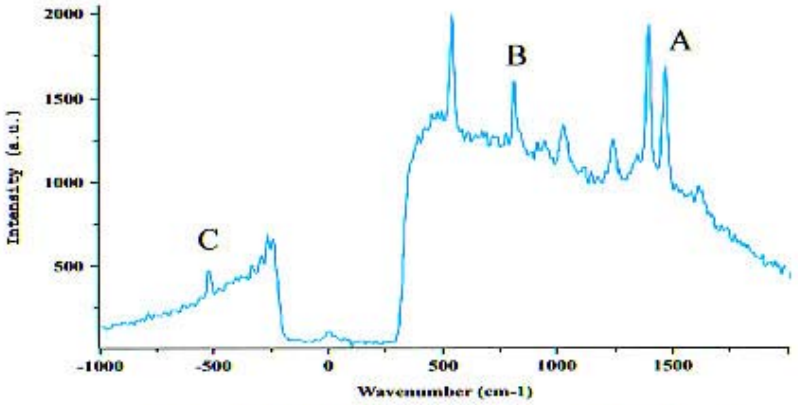

Near-field Phthalazine Raman spectrum

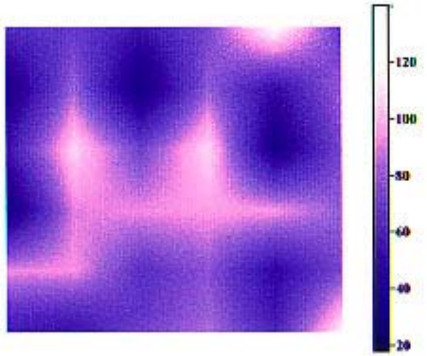

(A) map of 1465 cm^{-1} peak

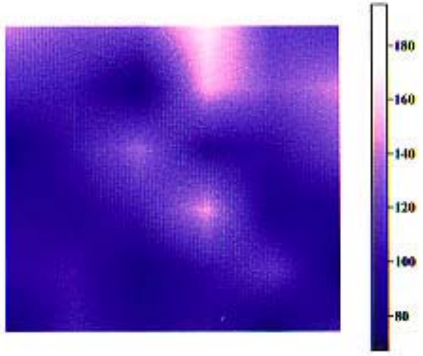

(B) map of 810 cm^{-1} peak

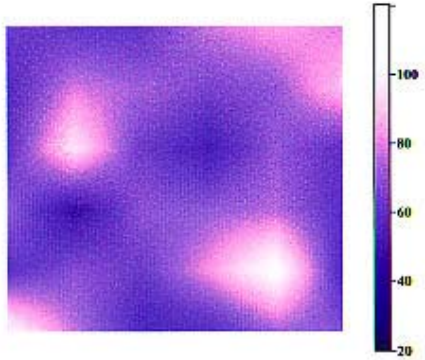

(C)map of -530 cm^{-1} peak

Tay et al -- hot spots are seen in near-field SERS as well

Far-Field Raman Maps of R6G on Ag Films

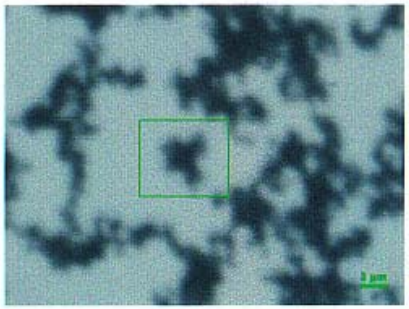

Optical image of Ag films

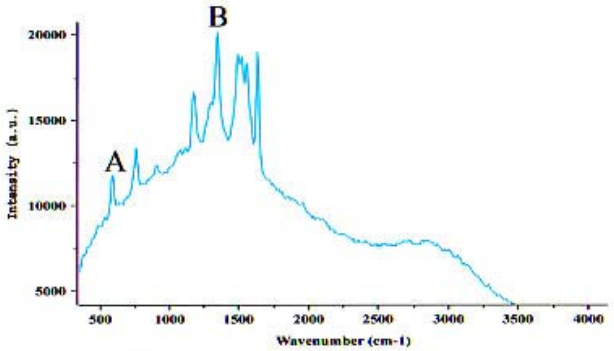

Far-field R6G Raman spectrum

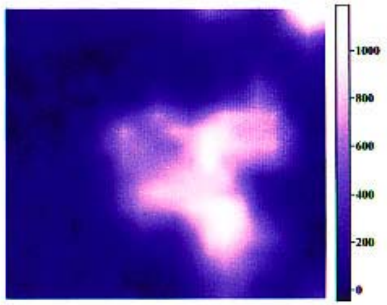

A

Far-field Raman map of peak 750 cm^{-1}

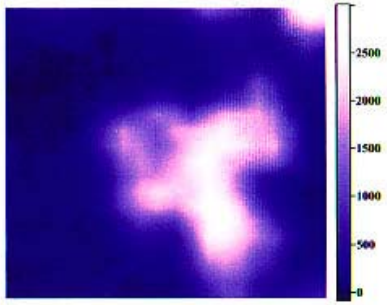

B

Far-field Raman map of peak 1340 cm^{-1}

The near-field images (shown previously) contrasts with far-field image (Tay et al.) above. The hot spots are averaged out.

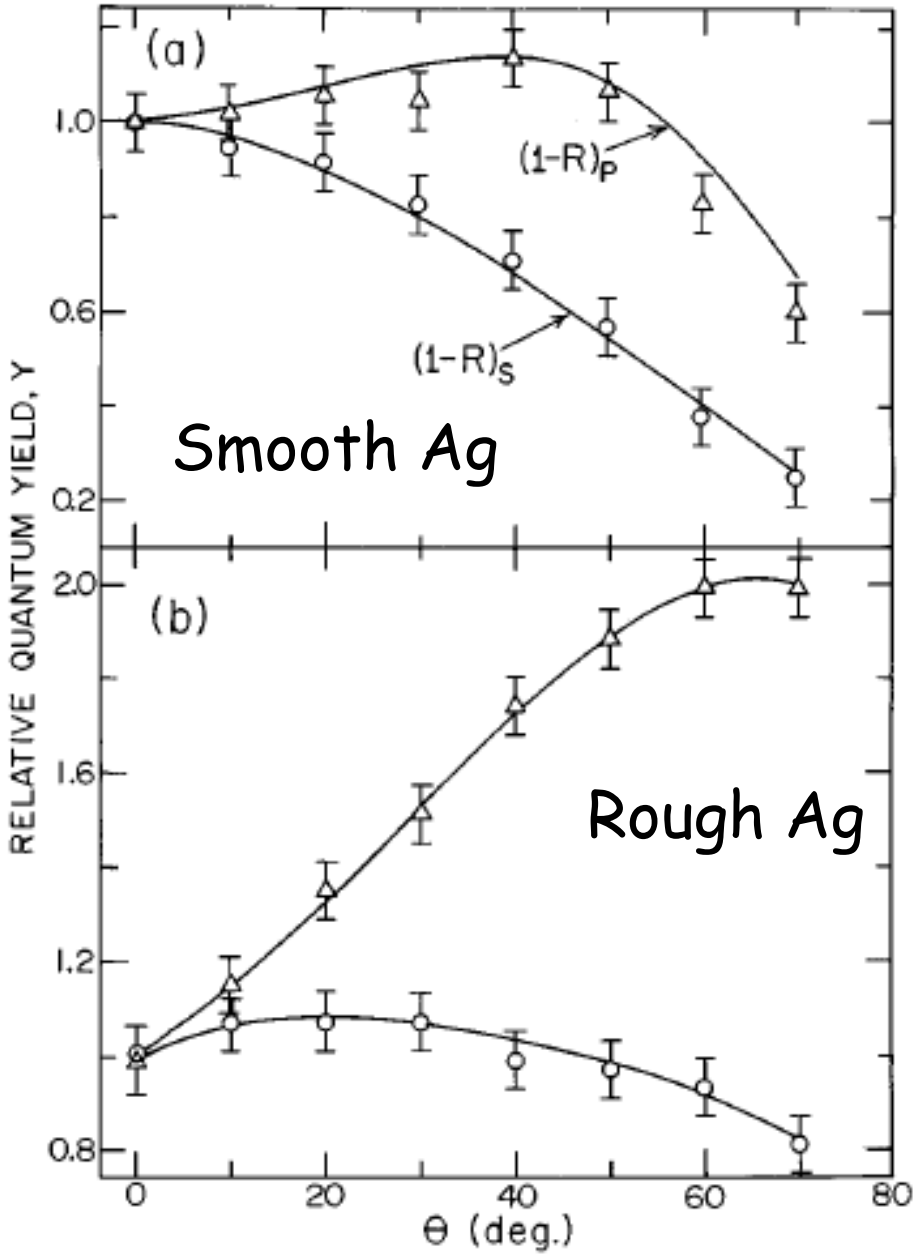
(a)
(b)
Smooth Ag
Rough Ag
(1-R)P
(1-R)S
RELATIVE QUANTUM YIELD, Y
Θ (deg.)
1.0
0.6
0.2
2.0
1.6
1.2
0.8
0
20
40
60
80

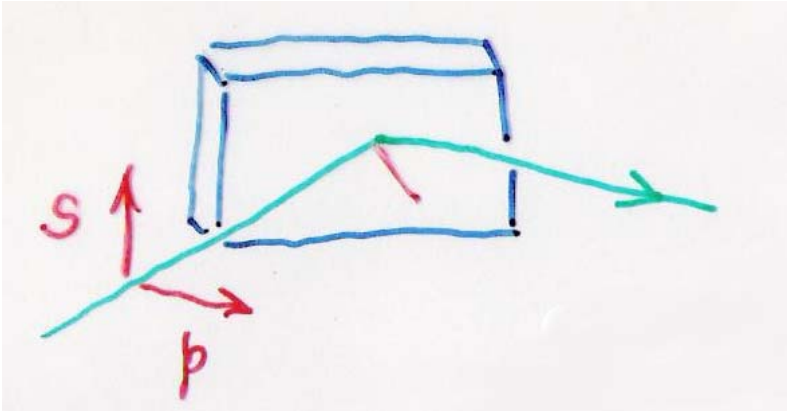
s
p

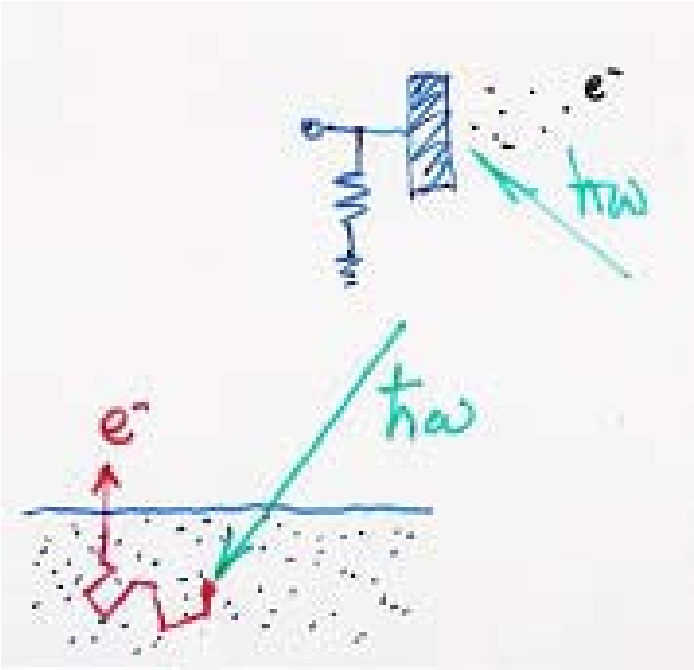
e⁻
ħω
e⁻
ħω

1-Photon, rough Ag

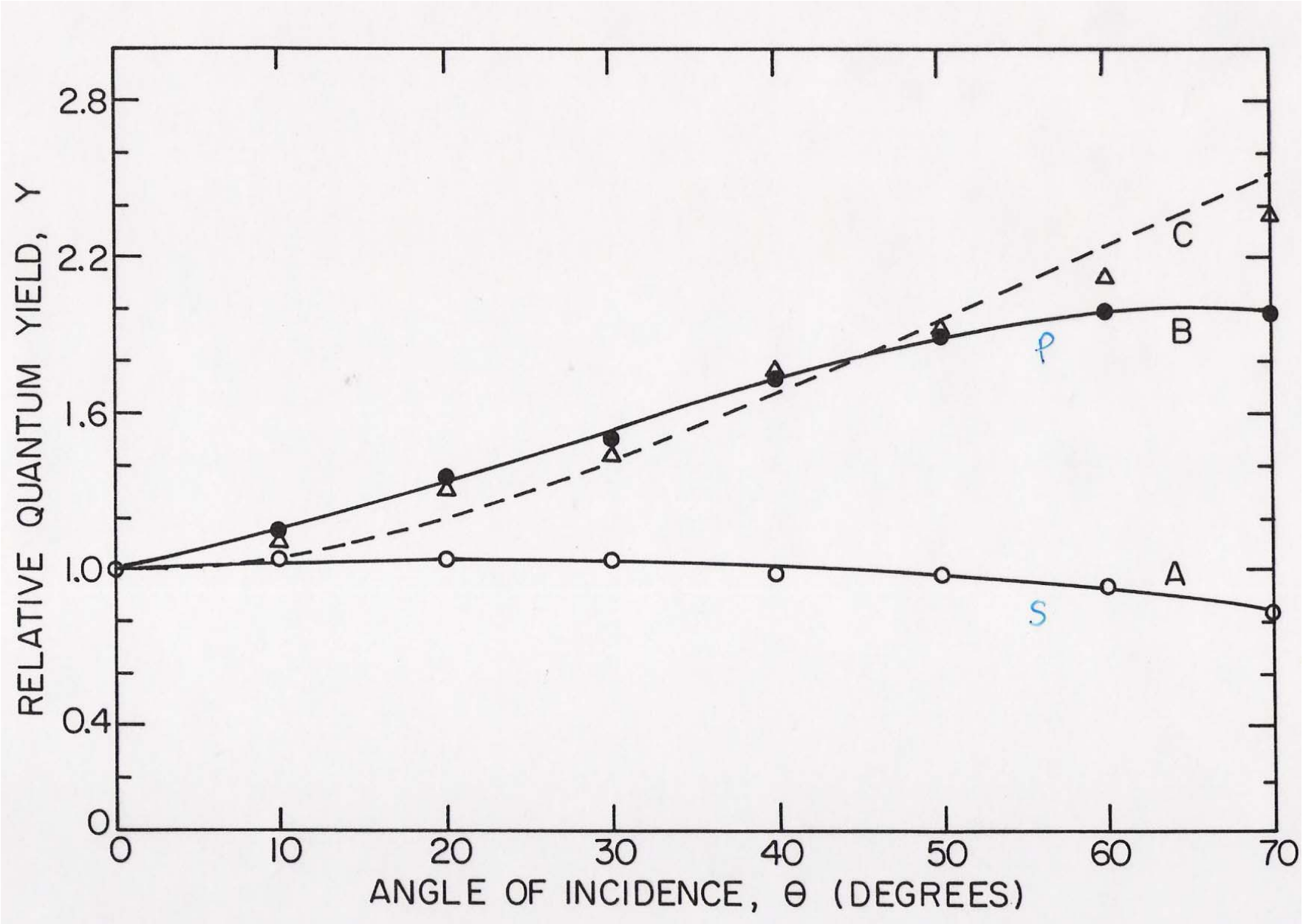

2-photon, rough Ag

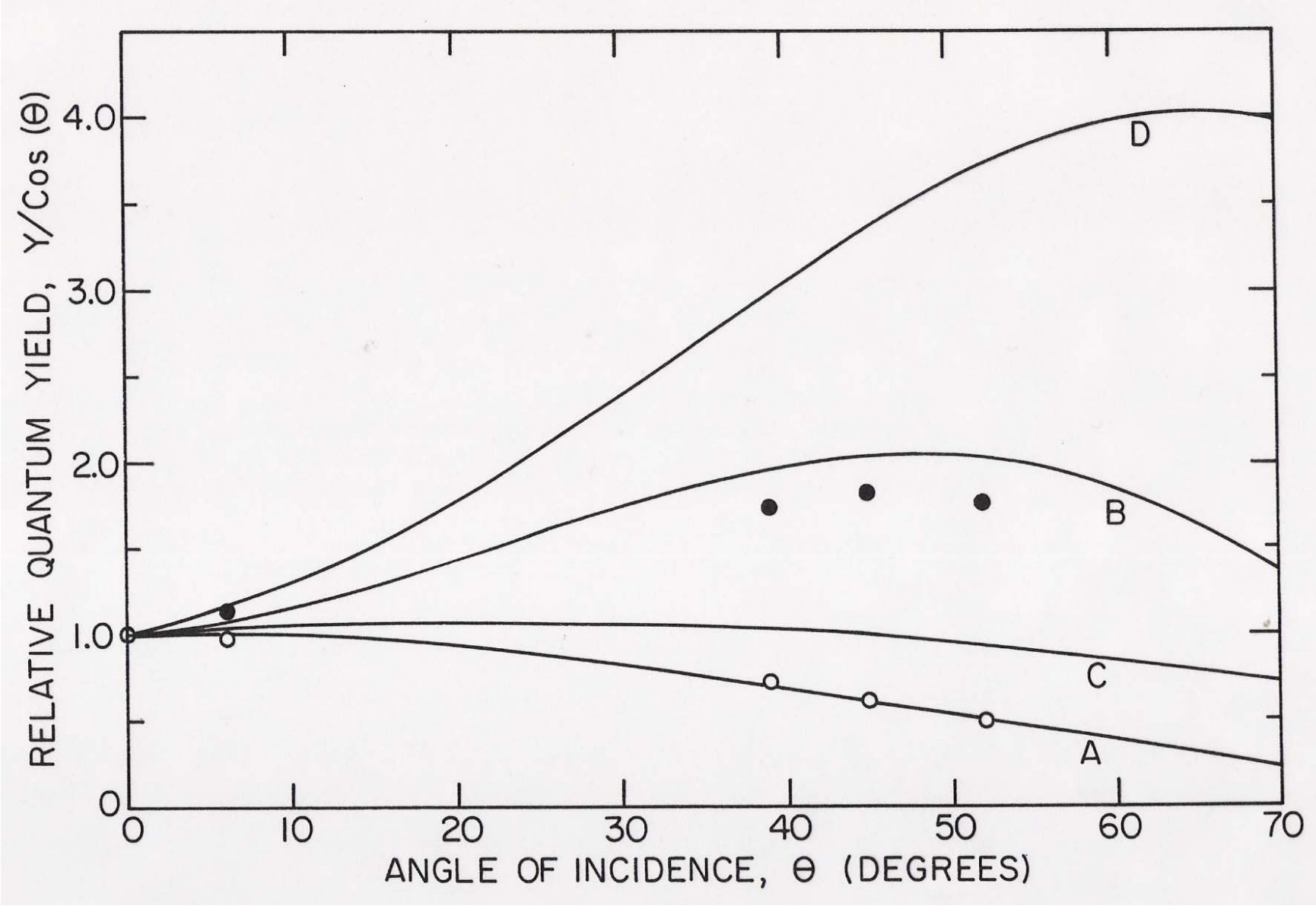

The ratio $\frac{Y_P}{Y_S} = \frac{(1-R_P)}{(1-R_S)}$ for 1-photon

both for rough & smooth surfaces.

and $\frac{Y_P}{Y_S} = \left[\frac{(1-R_P)}{(1-R_S)}\right]^2$ for 2-photon excitation.

This implies that for a rough film:

$$Y^{1\text{-ph}} \propto (1-R)\, f(\theta)$$

$$Y^{2\text{-ph}} \propto (1-R)^2\, f(\theta)$$

Since $f(\theta)$ doesn't appear as a square

$\Rightarrow$ it is associated with the emissive step, hence θ dependence is mysterious since it implies that the electron "remembers" directionality of the photon's $\vec{k}$.

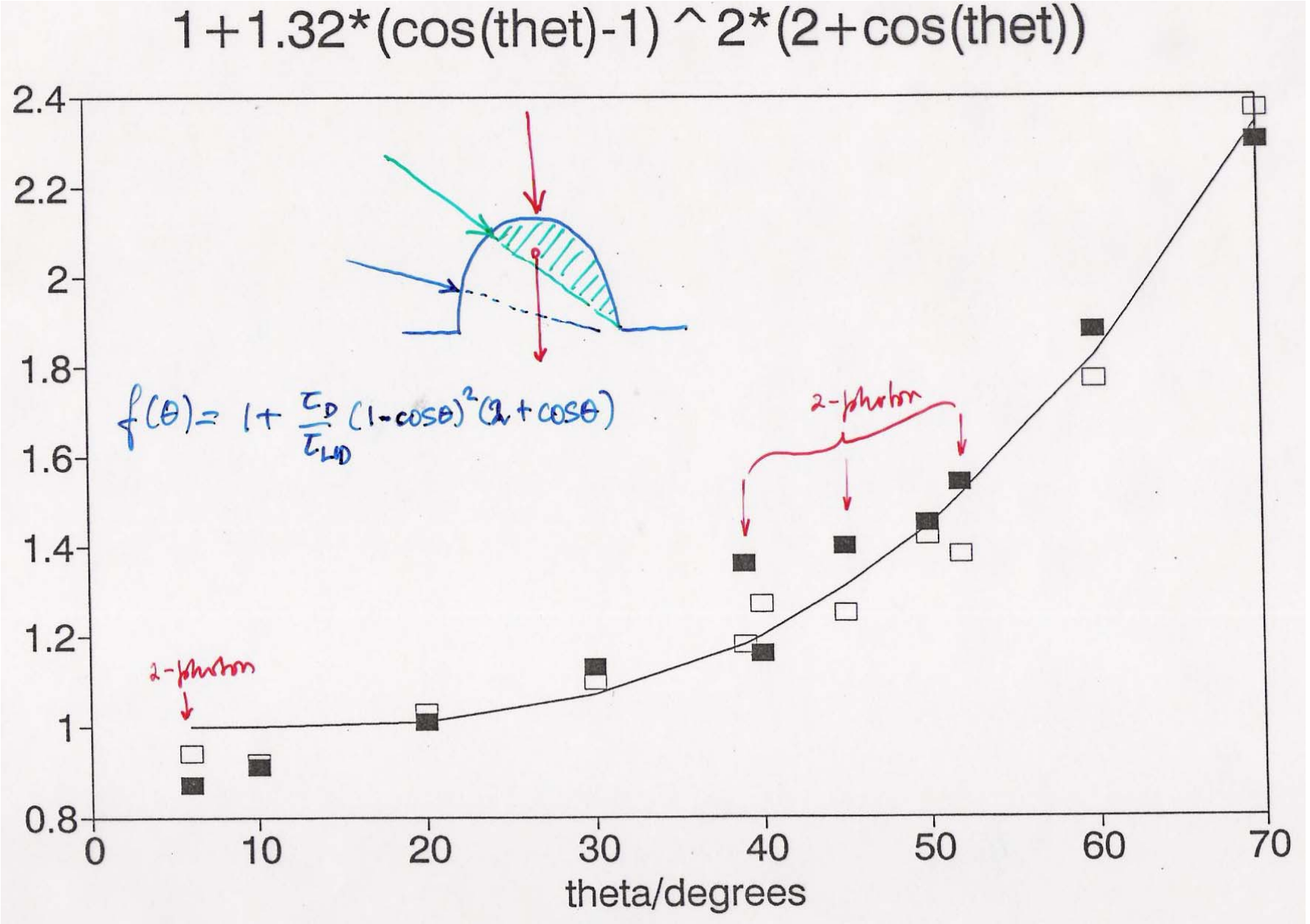
1+1.32*(cos(thet)-1) ^ 2*(2+cos(thet))
2.4
2.2
2
1.8
1.6
1.4
1.2
1
0.8
0
10
20
30
40
50
60
70
theta/degrees
f(θ) = 1 + τD/τLAD (1-cosθ)²(2+cosθ)
2-photon
2-photon

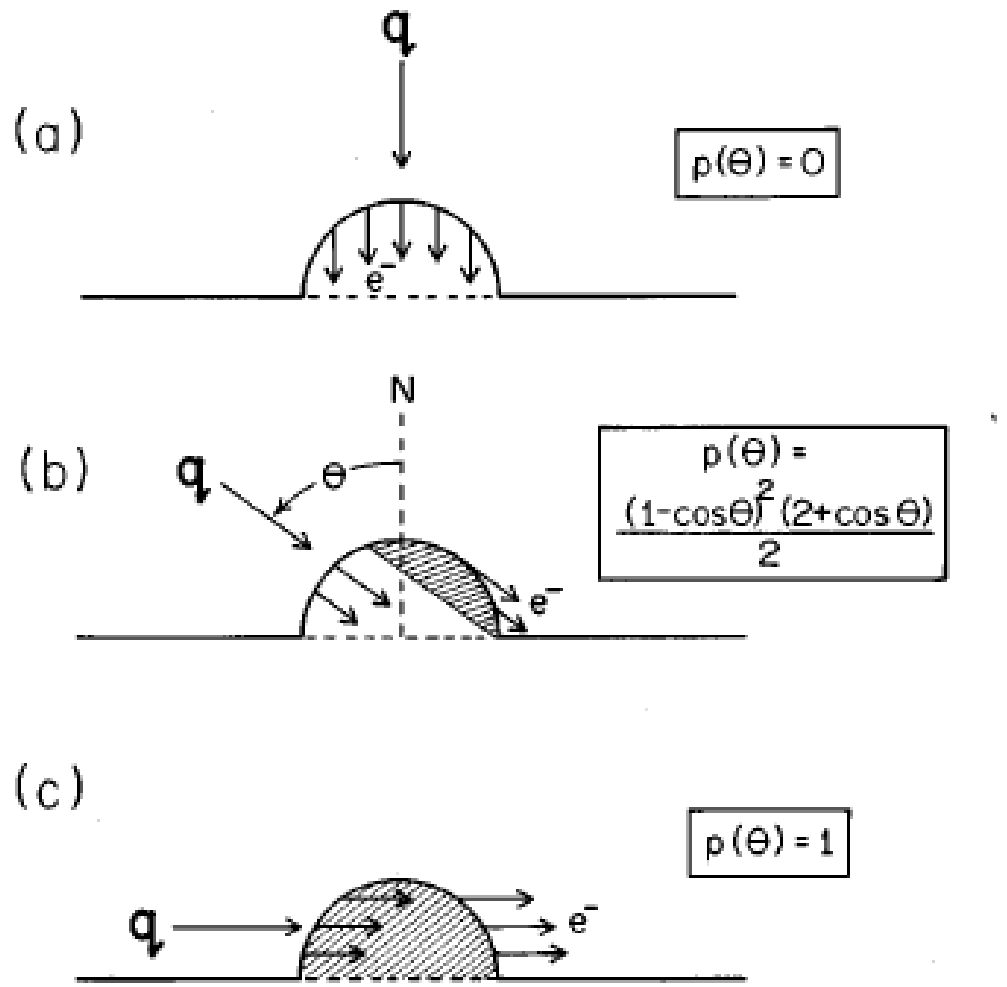

FIG. 5. The volume fraction of a semispherical protrusion from which electrons moving along the wave vector can reach the metal-vacuum interface.

Doppler effect

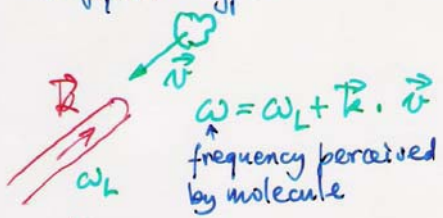

$\omega = \omega_L + \vec{k} \cdot \vec{v}$

↑ frequency perceived by molecule

$|\vec{k}| = \frac{2\pi}{\lambda}$

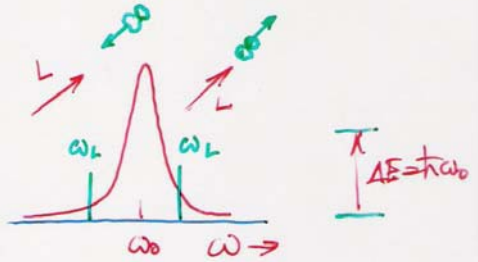

$\omega \rightarrow \omega_0$ $\quad$ $\omega \rightarrow \omega_0$

$\omega = \omega_L + |\vec{k} \cdot \vec{v}|$ $\quad$ $\omega = \omega_L - |\vec{k} \cdot \vec{v}|$

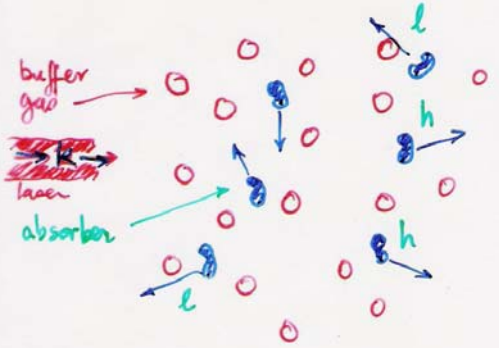

if collision rate is greater in the excited state (e.g. because cross section increases)

h drifts ←

l drifts →

Same sort of thing for electrons in metals except that metals are characterized by broad energy bands

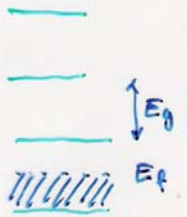

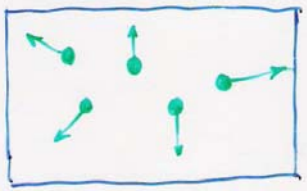

no net current ∴ electrons are moving in all directions

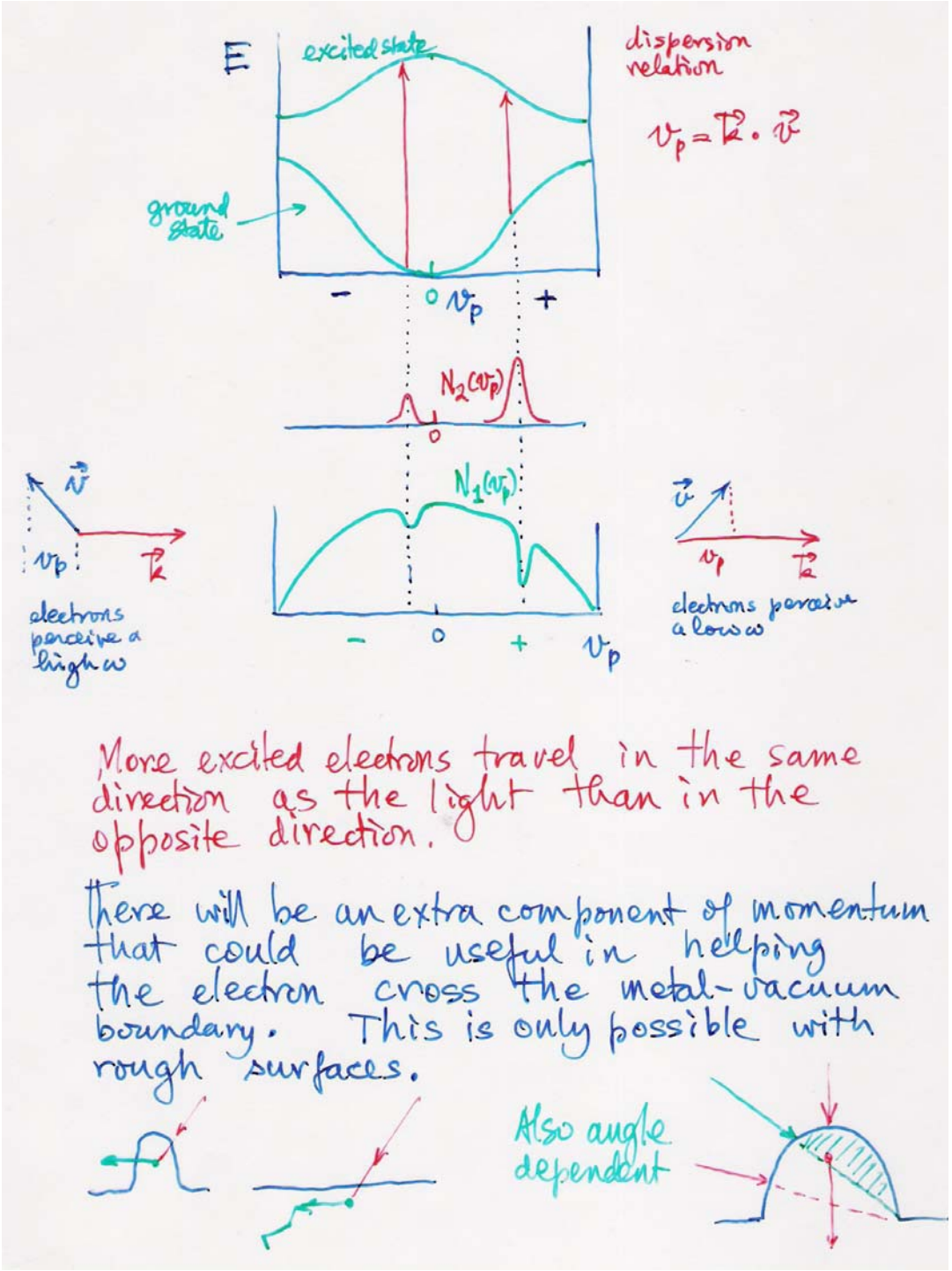

V.SShalaev et al. Phys. Lett. A 169 205 (1992).

Theory is based on pioneering work of Stockman et al.

Apparatus

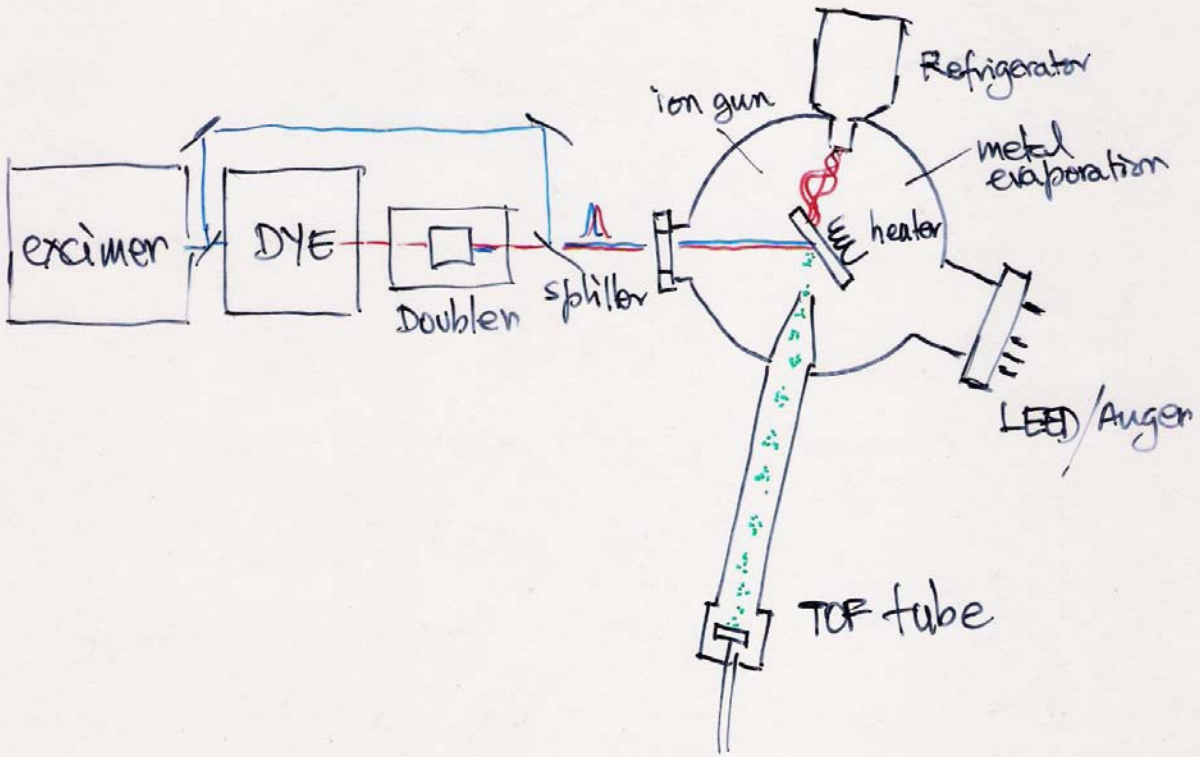

field enhancement increases
cross-section for 2-photon processes
locally on surface.

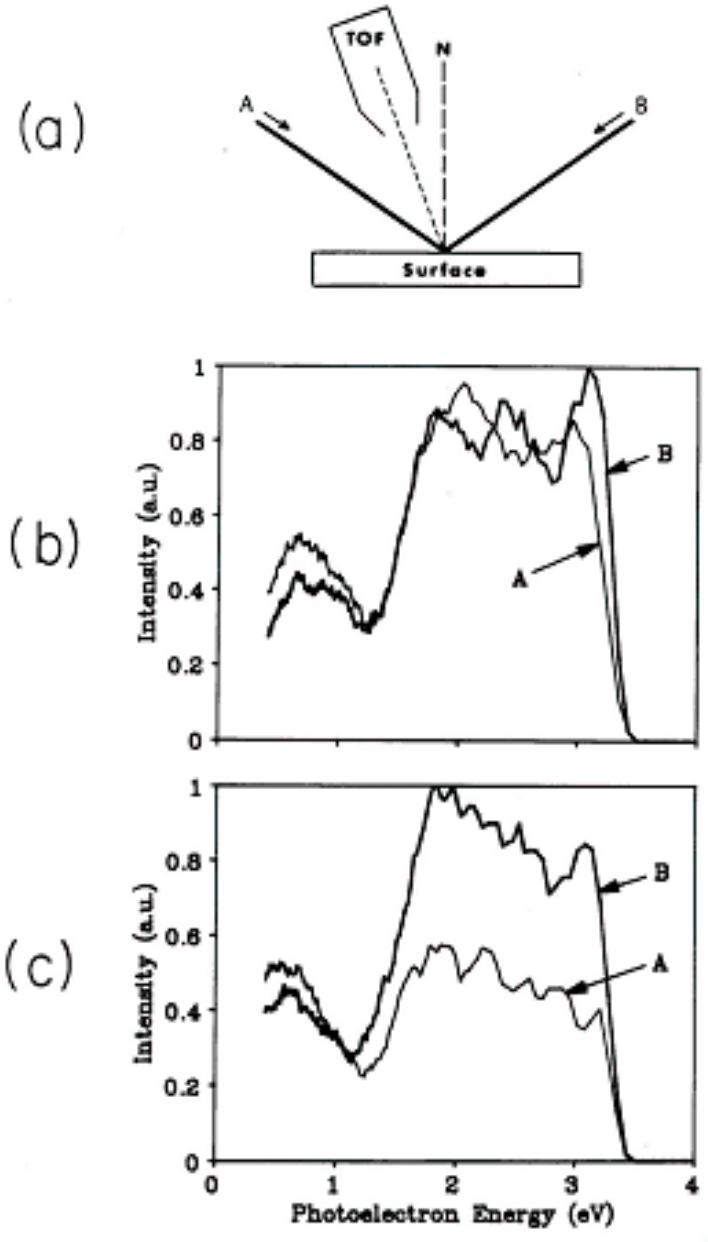

smooth

rough

The Rebirth of SERS as a single-molecule effect

Shuming Nie and Steven R. Emory

SCIENCE **275**, 1102 1997

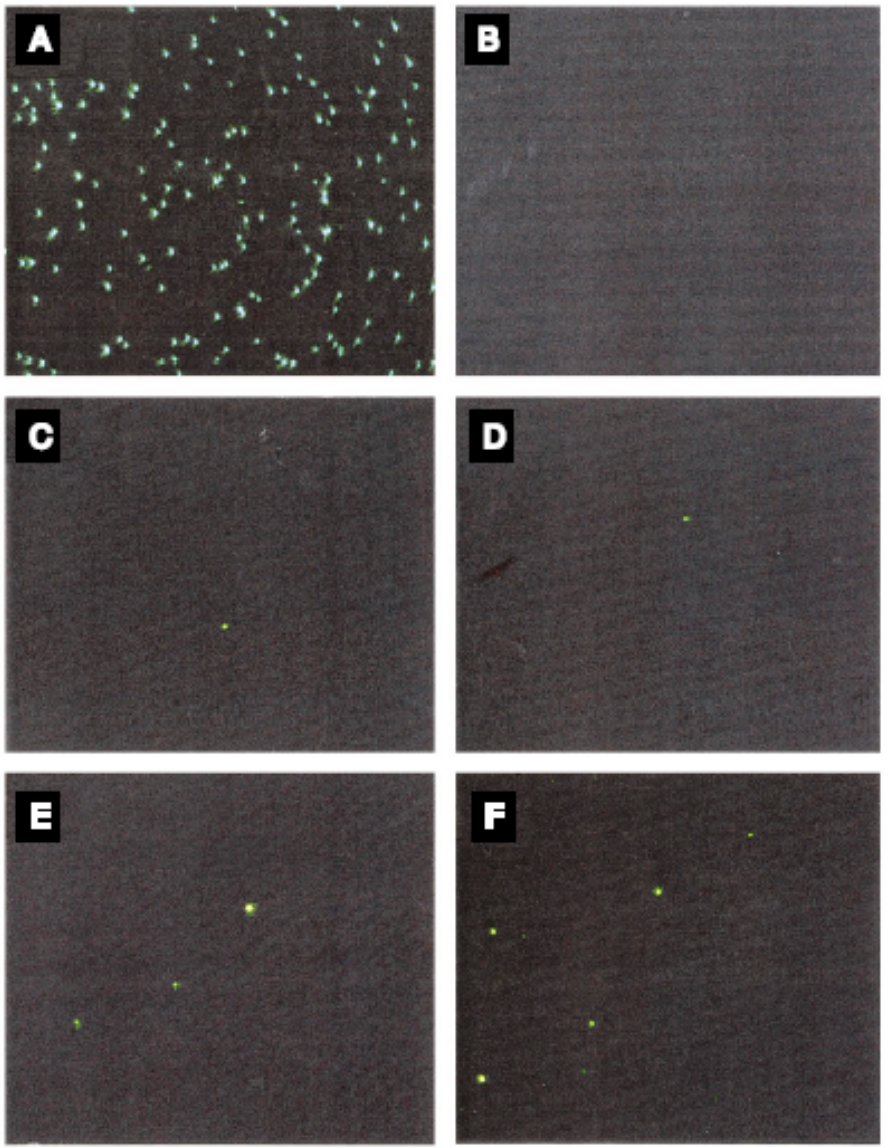

Fig. 1. Ag nanoparticles imaged with evanescent-wave excitation. Total internal reflection of the laser beam at the glass-liquid interface was used to reduce the laser scattering background. The instrument setup for evanescent-wave microscopy was adapted from Funatsu *et al.* (*11*). The images were directly recorded on color photographic film (ASA-1600) with a 30-s exposure by a Nikon 35-mm camera attached to the microscope. (**A**) Unfiltered photograph showing scattered laser light from all particles immobilized on a polylysine-coated surface. (**B**) Filtered photographs taken from a blank Ag colloid sample (incubated with 1 mM NaCl and no R6G analyte molecules). (**C**) and (**D**) Filtered photographs taken from a Ag colloid sample incubated with 2×10^{-11} M R6G. These images were selected to show at least one Raman scattering particle. Different areas of the cover slip were rapidly screened, and most fields of view did not contain visible particles. (**E**) Filtered photograph taken from Ag colloid incubated with 2×10^{-10} M R6G. (**F**) Filtered photograph taken from Ag colloid incubated with 2×10^{-9} M R6G. A high-performance bandpass filter was used to remove the scattered laser light and to pass Stokes-shifted Raman signals from 540 to 580 nm (920 to 2200 cm^{-1}). Continuous-wave excitation at 514.5 nm was provided by an Ar ion laser. The total laser power at the sample was 10 mW. Note the color differences between the scattered laser light in (A) and the red-shifted light in (C) through (F).

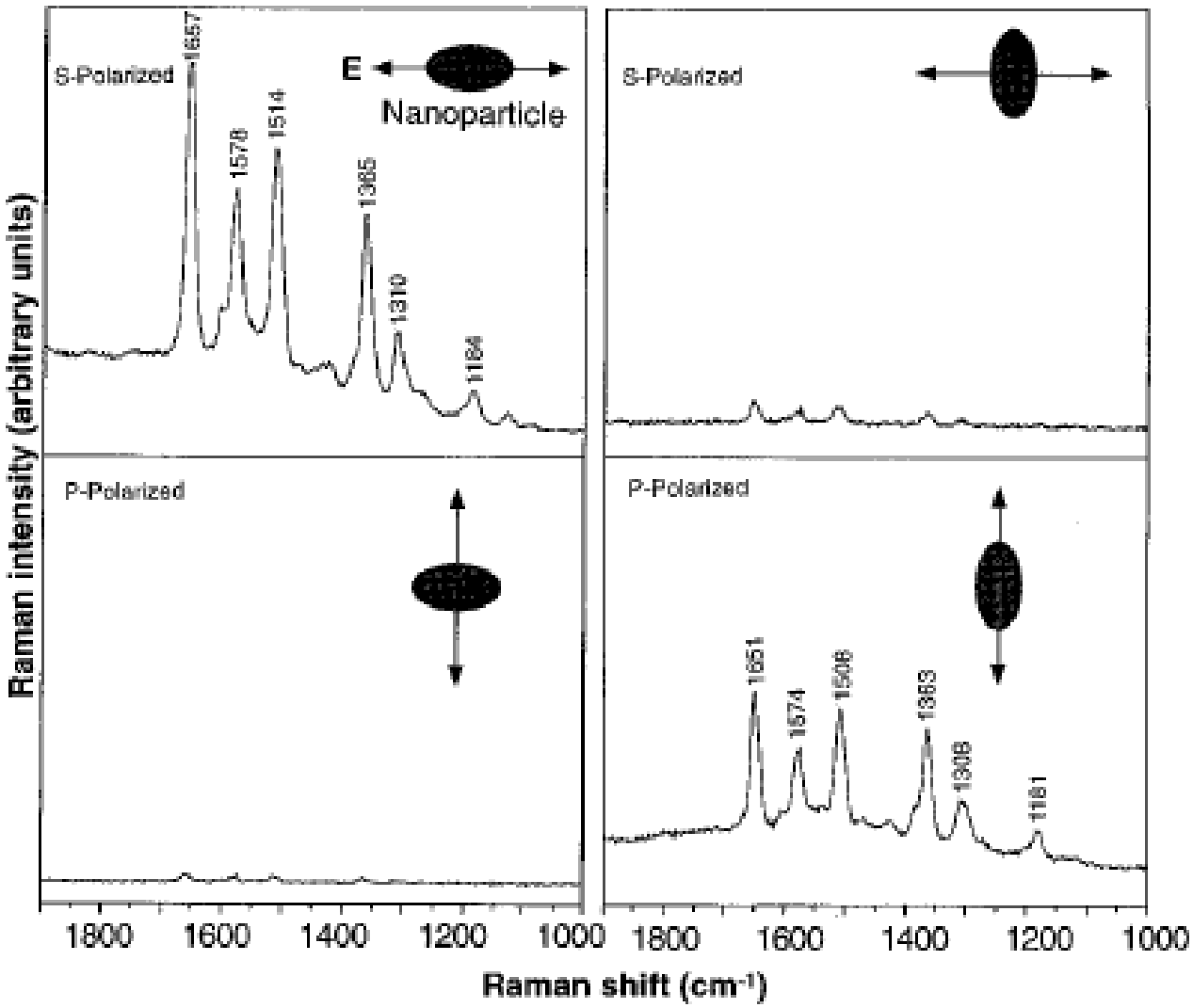

Fig. 3. Surface-enhanced Raman spectra of R6G obtained with a linearly polarized confocal laser beam from two Ag nanoparticles. The R6G concentration was 2×10^{-11} M, corresponding to an average of 0.1 analyte molecule per particle. The direction of laser polarization and the expected particle orientation are shown schematically for each spectrum. Laser wavelength, 514.5 nm; laser power, 250 nW; laser focal radius, ~250 nm; integration time, 30 s. All spectra were plotted on the same intensity scale in arbitrary units of the CCD detector readout signal.

Some features of Single Molecule SERS:

1. Low density of hot molecules
2. Early saturation with coverage – addition of adsorbate doesn't increase SERS signal.
3. The higher the adsorbate dose the more hot particles appear

The effect is not a single-particle effect

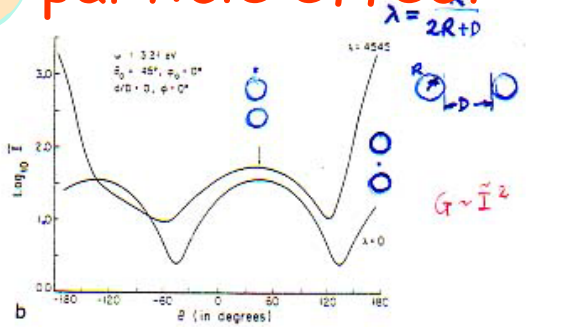

Fig. 3. (a) Plot of $\bar{I}$ (on a log scale) versus polar angle of observation point, θ, for the 2-sphere system $\lambda = 0.4545$ and the isolated sphere $\lambda = 0$. The external frequency $\omega = 3.48$ eV is at resonance for the isolated sphere and also very close to the upper resonance of the 2-sphere system. Arrow in figure is along the direction of the external field, in this case 45°. (b) Same as (a) but for $\omega = 3.21$ eV, the lower resonance frequency of the 2-sphere system with $\lambda = 0.4545$.

Aravind, Nitzan & Metiu
Surf. Sci 110, 189 (1981)

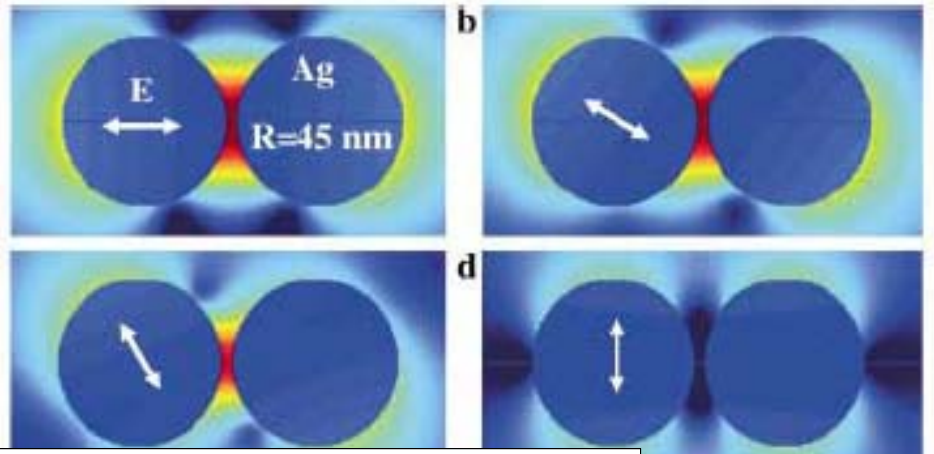

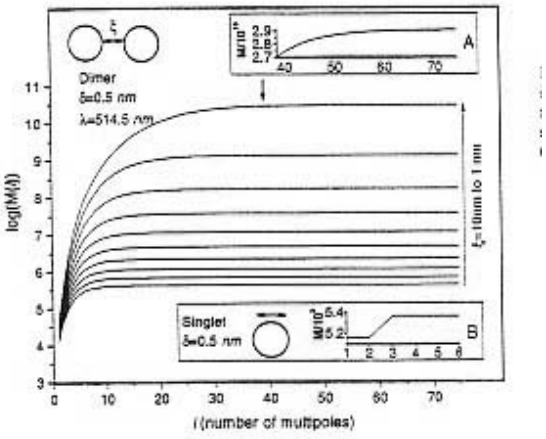

HongXing Xu, thesis with Käll

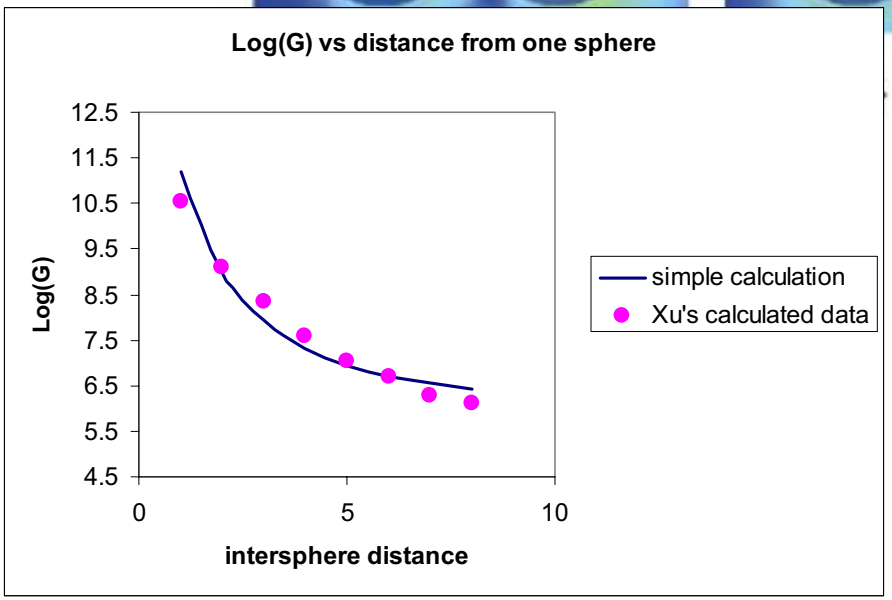

The field at the interstitial point between two spheres can be so great as to produce an enhancement as large as 10^{11}. Most small clusters will possess interstitial points where the enhancement will be unusually high.

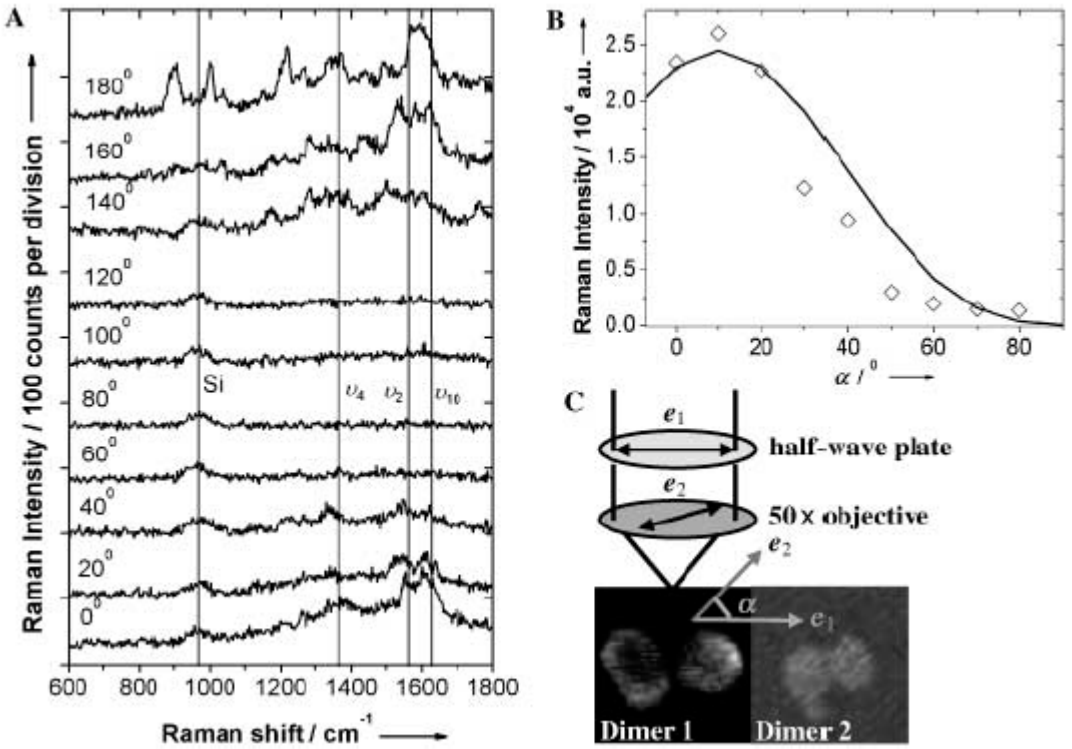

Kall, Xu, ChemPhysChem

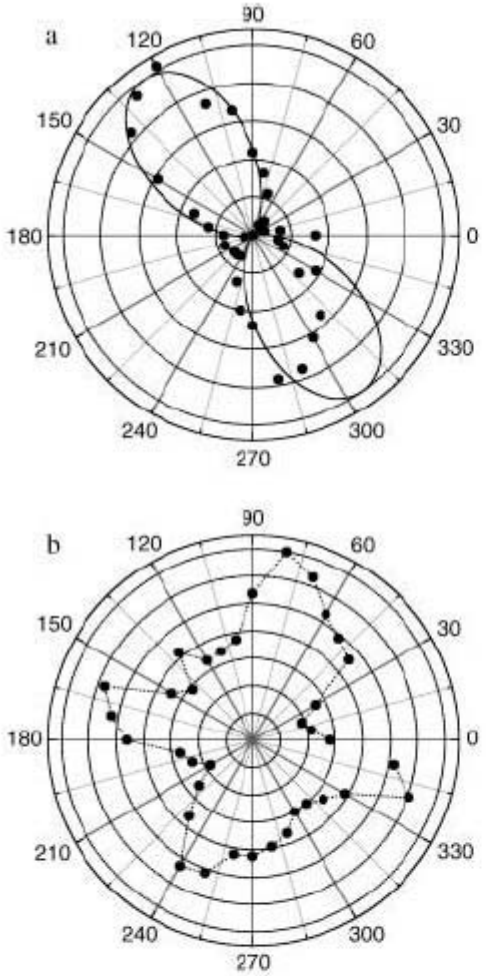

Figure 3. *Polar plots of the Raman intensity of a) spot A and b) spot C in Figure 2 versus polarization angle α (●), and fit (——) to a $\cos^4(\alpha - \alpha_o)$ dependency in a). The Raman intensity scale (a.u.) corresponds to 500 and 2000 counts per division in a) and b), respectively.*

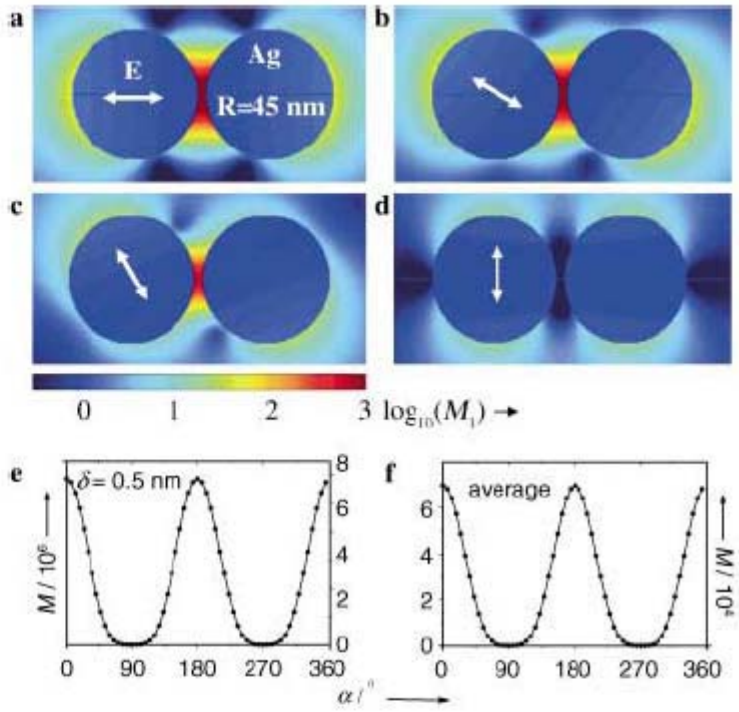

Figure 4. *Local intensity enhancement $M_1 = [E_{loc}/E_o]^2$ in logarithmic scale in a plane through the centers of the Ag spheres and perpendicular to the incident wave-vector **k** versus incident polarization: a) 0°, b) 30°, c) 60° and d) 90°. The arrows represent the different polarizations. In e), we show the SERS enhancement factor $M = M_1^2$ (dots) as a function the incident polarization α for a point in the nanogap located at the dimer axis δ = 0.5 nm away from one spherical surface, and fit (solid line) to a $\cos^4(\alpha)$ dependency. In f), we show M (●) averaged over all points δ = 0.5 nm outside the Ag sphere surfaces versus α, and fit (——) to a $\cos^4(\alpha)$ dependency. The radius R = 45 nm corresponds to the average size of the Ag nanoparticles used in the experiment while the separation distance d = 5.5 nm corresponds to the diameter of a Hb molecule. The incident wavelength is 514.5 nm in all cases. Calculations were performed using a dielectric function for Ag based on experimental data.*[15]

This explanation accounts for all of the major observations reported in single-molecule SERS experiments:

1. Low density of hot molecules -- only aggregates with highly effective hot spots and only molecules residing in hot spots are active.

2. Early saturation with coverage -- once the hot spot is occupied further adsorption doesn't contribute significantly to the Raman signal. The high field gradients may actually draw molecules with permanent or induced dipoles into the hot spot causing the hot spots to be preferentially occupied to an extent exceeding simple probability.

3. The higher the adsorbate dose the more hot particles appear -- the probability that a molecule will land in a hot spot increases with increasing dose.